Tidally-generated internal waves and mixing in the ocean

Sonya Legg
Princeton University

Tides and winds provide mechanical energy for ocean mixing

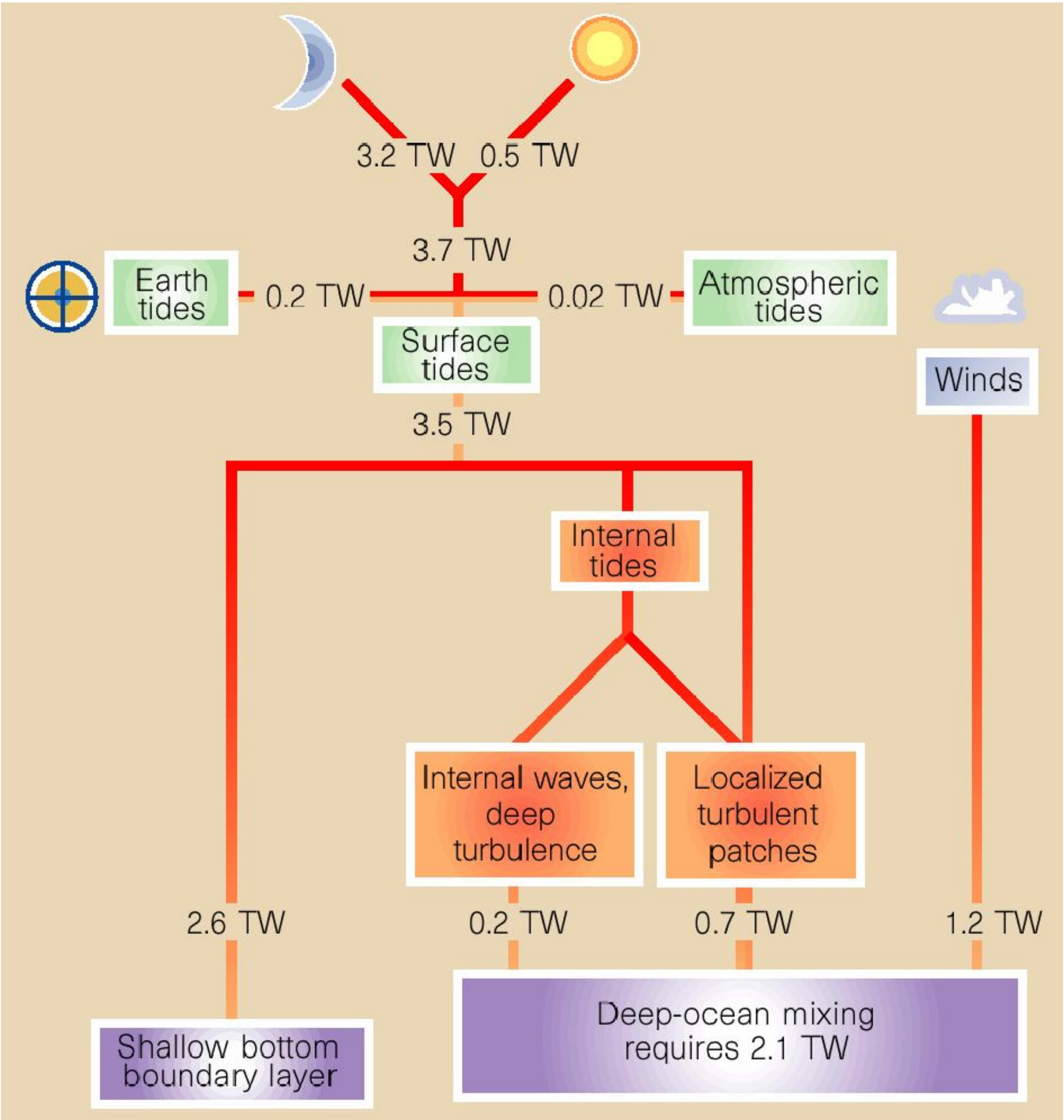

Tides supply ~50% of energy used for mixing in open ocean. Much of this energy passes through the internal wave field.

Coarse resolution ocean climate models must include parameterizations of tidal mixing.

Munk and Wunsch, 1998

Internal wave driven mixing pathways

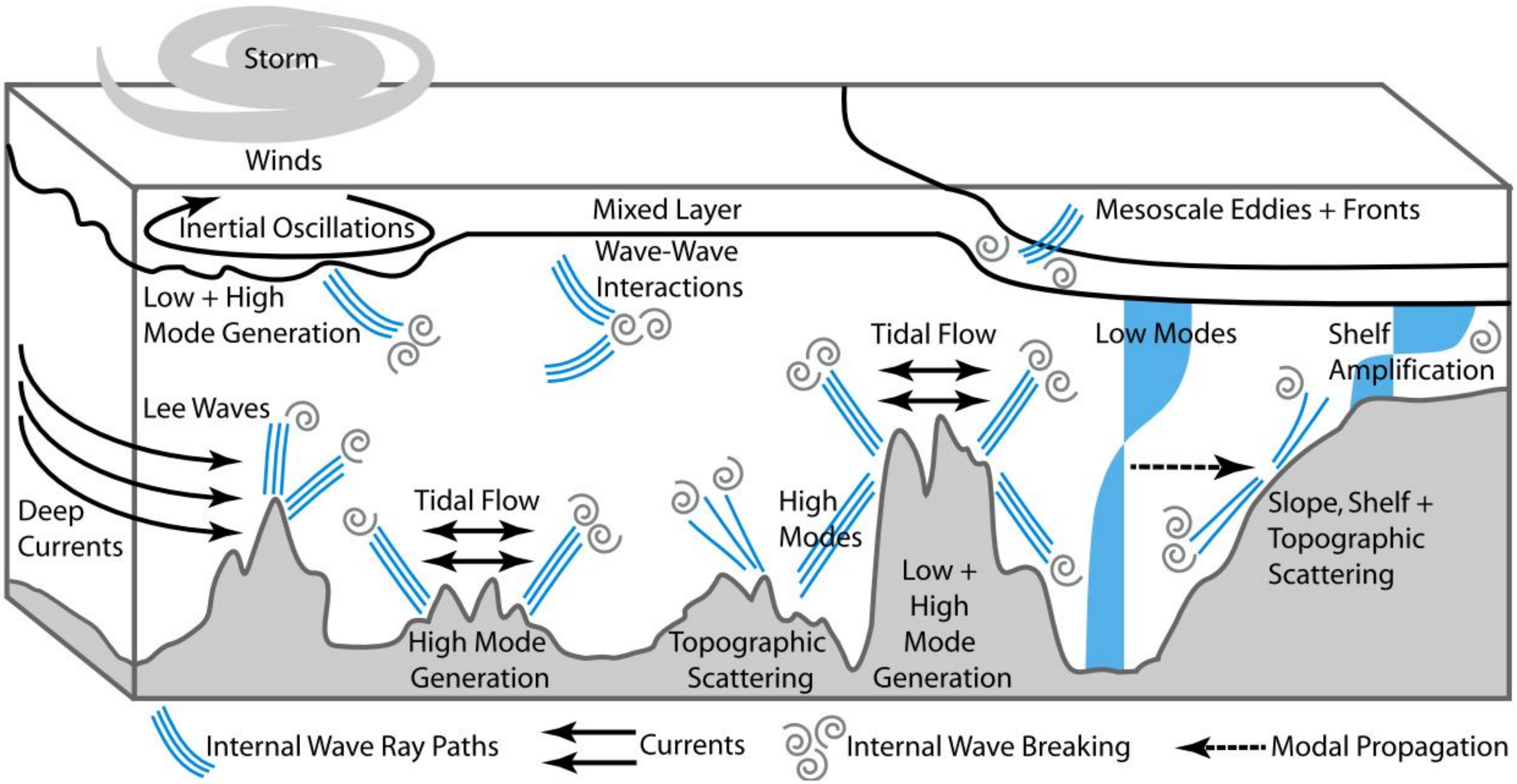

Winds, tides and subinertial flow generate internal waves, which propagate, and eventually break. Some of the wave energy leads to mixing across density surfaces (diapycnal mixing), both near and far from the wave generation site.

MacKinnon et al, 2017, BAMS
Internal wave driven mixing Climate Process Team

An energetically consistent framework for parameterizing tidal mixing

Local dissipation

St Laurent et al, 2002

$$\varepsilon = \frac{1}{\rho}\boxed{E(x,y)}\cdot\boxed{q}\cdot\boxed{F(z)}$$

Rate of energy conversion from barotropic tide to baroclinic per unit area.

Fraction of local dissipation.
Set (arbitrarily) to 1/3 in current implementations

Vertical structure function
$\int_{-H}^{0} F(z)dz = 1$

Exponential decay with (arbitrary) constant vertical scale in current implementations

Mixing efficiency

$$\kappa = \varepsilon \frac{\boxed{\Gamma}}{N^2}$$

(Osborn, 1980)

Local and remote dissipation: globally require

$$\int \varepsilon dV = \frac{1}{\rho}\int E(x,y)dxdy$$

Outline

$$\kappa = \varepsilon \frac{\Gamma}{N^2} \qquad \varepsilon = \frac{1}{\rho} E(x,y) \cdot q \cdot F(z)$$

Break down the components of this parameterization and its improvements

- Tracer diffusivity expressed in terms of turbulent kinetic energy dissipation (Osborn, 1980): $\kappa = \varepsilon \frac{\Gamma}{N^2}$
- Energy conversion from barotropic to baroclinic tides: $E(x,y)$
- Local breaking of internal tides: $q, F(z)$
- Farfield breaking of internal tides: $(1-q)$
- Toward a global parameterization: $\kappa(x,y,z,t)$
- Impact of tidally-driven mixing parameterizations on ocean circulation and climate

Tracer diffusivity from turbulent kinetic energy budget (Osborn, 1980)

TKE eqn:
$$\left(\frac{\partial}{\partial t} + \bar{u}_j \frac{\partial}{\partial x_j}\right) \frac{\overline{u_i'^2}}{2} = \frac{\partial}{\partial x_j}\left(F_{i,j}\right) - \epsilon + P + B$$

$$F_{i,j} = \left(-\frac{1}{\rho_0}\overline{u_i' p'}\delta_{i,j} + \nu \frac{\partial}{\partial x_j}\frac{\overline{u_i'^2}}{2} - \overline{u_j' u_i' u_i'}\right)$$ Transport

$$\epsilon = \nu \overline{\left(\frac{\partial u_i'}{\partial x_j}\right)^2}$$
Dissipation

$$P = -\overline{u_j' u_i'}\frac{\partial}{\partial x_j}\bar{u}_i$$
Shear production

$$\mathrm{B} = \overline{b' w'}$$
Buoyant production

For steady state, closed volume: $\epsilon = P + B$

Define flux Richardson number
$R_f = -\frac{B}{P}$

$B = \overline{b' w'} = -\kappa_b \frac{\partial \bar{b}}{\partial z} = -\kappa_b N^2$ where κ_b is the eddy diffusivity of buoyancy.

$$\boxed{\kappa_b = \frac{R_f}{(1-R_f)}\frac{\epsilon}{N^2} = \Gamma \frac{\epsilon}{N^2}}$$ where Γ = mixing efficiency.

For stratified turbulence, $\Gamma \approx 0.2$ *(subject of active research, see Chris Howland's poster).*

Energy conversion from barotropic to baroclinic tide: Governing parameters for tidal flow over topography

Topography: height *h*, width *L*, depth *H*
Flow: speed *U*, oscillation frequency ω
Others: coriolis *f*, buoyancy frequency *N*

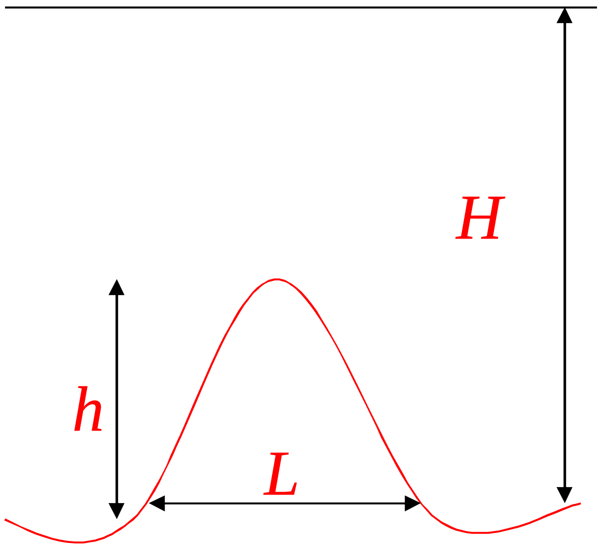

Nondimensional parameters

Wave slope
$$s = \frac{k}{m} = \left(\frac{\omega^2 - f^2}{N^2 - \omega^2} \right)^{1/2}$$

Topography — Relative steepness
$$\gamma = \frac{\nabla h}{s}$$

Relative height
$$\frac{h}{H}$$

Flow — Tidal excursion
$$R_L = \frac{U}{L\omega}$$

Froude numbers
$$Fr = \frac{U}{Nh} \qquad Fr_w = \frac{U}{C_p}$$

Garrett and Kunze, 2007

Generation of linear internal waves by flow over topography

3-dimensional inviscid Boussinesq equations, with buoyancy and rotation.

$$\frac{D\boldsymbol{u}}{Dt} + \boldsymbol{f} \times \boldsymbol{u} = -\frac{\nabla p}{\rho_0} + b\hat{\boldsymbol{k}}$$

$$\frac{Db}{Dt} = 0$$

$$\nabla . \boldsymbol{u} = 0$$

Consider perturbations about a state with oscillating horizontal flow:
$U(t)=U_0\cos(\omega t)$; stable linear stratification: $b = N^2 z$; and f=0 (for convenience).

$$\left(\frac{\partial}{\partial t} + U(t)\frac{\partial}{\partial x}\right)\boldsymbol{u}' = -\frac{\nabla p'}{\rho_0} + b'\hat{\boldsymbol{k}}$$

$$\left(\frac{\partial}{\partial t} + U(t)\frac{\partial}{\partial x}\right)b' + N^2 w' = 0$$

$$\nabla . \boldsymbol{u}' = 0$$

Bell, 1974

For flow over topography h(x), bottom boundary condition is: $w'(t,x) = U(t)\dfrac{dh}{dx}$

Weak topography approximation: boundary condition is applied at z=0 not z=h(x).

Internal tide generation schematic

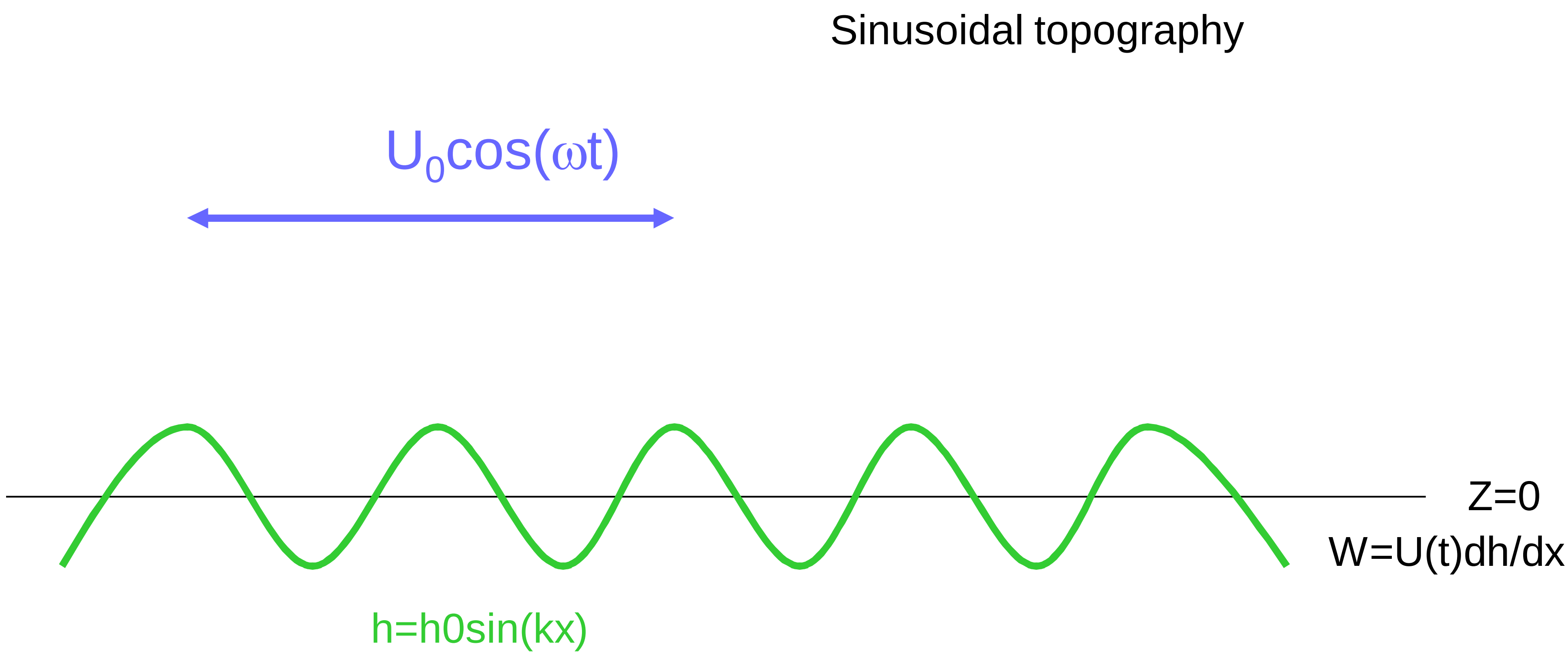

Acoustic limit

If $$\frac{\partial u'}{\partial t} >> U_0 \cos(\omega t) \frac{\partial u'}{\partial x} \rightarrow \frac{U_0 k}{\omega} << 1$$

Then we can simplify equations:

$$\boxed{\begin{aligned} \frac{\partial}{\partial t}\boldsymbol{u}' &= -\frac{\nabla p'}{\rho_0} + b'\hat{\boldsymbol{k}} \\ \frac{\partial}{\partial t} b' + N^2 w' &= 0 \\ \nabla . \boldsymbol{u}' &= 0 \end{aligned}}$$

Wave equation:

$$\frac{\partial^2}{\partial t^2}\nabla^2 w' + N^2 \nabla_H{}^2 w' = 0 \qquad w(z=0) = h_0 U_0 \cos(\omega t) k \cos(kx)$$

Acoustic limit solutions

$$w = \frac{1}{2} U_0 h_0 k \,\mathrm{Re}\left[\exp(i(kx + mz + \omega t)) + \exp(i(kx - mz - \omega t))\right]$$

Leftward propagating wave

Net wave

Rightward propagating wave

U_0 =0.2m/s,
λ_x=10/3km,
N=2e-3/s.

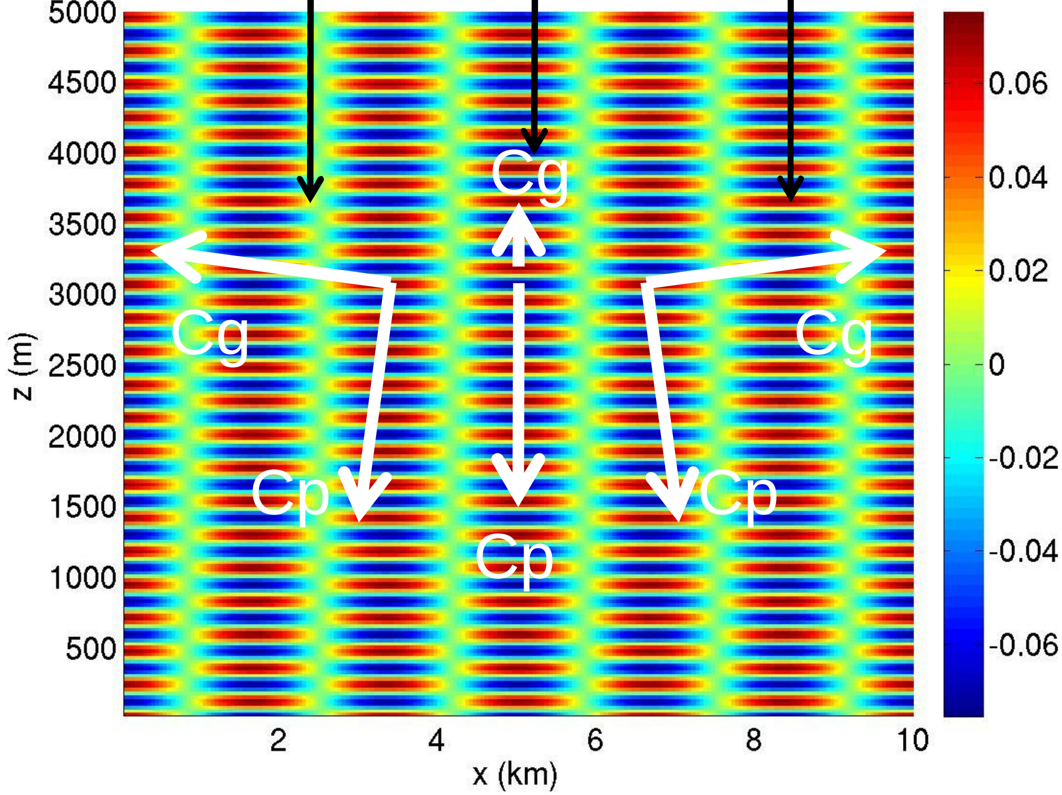

W (m/s), snapshot

Satisfies boundary conditions, and has upward group velocity

Acoustic limit energy flux <w'p'>:

$$E_f = \frac{1}{4} \rho_0 \omega^{-1} \left[\left(N^2 - \omega^2\right)\left(\omega^2 - f^2\right) \right]^{1/2} k U_0^{\,2} h_0^{\,2}$$

Full linear internal tide solution (Bell (1974) solution)

$$w = \frac{1}{2}\sum_{n=1}^{n_N} n\omega J_n\left(\frac{kU_0}{\omega}\right)h_0 \,\mathrm{Re}\left[\exp(i(k\zeta - mz - n\omega t)) + \exp(i(k\zeta + mz + n\omega t))\right]$$

$$\zeta = x - \frac{U_0}{\omega}\sin(\omega t)$$

$J_n =$ Bessel function of order n

Solution consists of fundamental frequency ω and higher harmonics nω

$$E_f = \rho_0 \sum_{n=1}^{n_N} n\omega\left[\left(N^2 - n^2\omega^2\right)\left(n^2\omega^2 - f^2\right)\right]^{1/2} k^{-1} J_n^{\,2}\left(\frac{U_0 k}{\omega}\right)h_0^2$$

where n_N is the largest integer < N/ω

For small kU/ω $$J_n\left(\frac{kU_0}{\omega}\right) \approx \left(\frac{kU_0}{2\omega}\right)^n \Big/ n$$

So if kU/ω<<1, then fundamental dominates and

$$E_f \approx \frac{1}{4}\rho_0\omega^{-1}\left[\left(N^2 - \omega^2\right)\left(\omega^2 - f^2\right)\right]^{1/2} kU_0^{\,2}h_0^{\,2} \qquad \approx \tfrac{1}{4}NkU_0^2h_0^2$$

for $N \gg \omega \gg f$

Barotropic to baroclinic energy conversion: comparison with observations

$$E(x,y)=\frac{1}{2}\rho_0 N_b k h^2\langle u^2\rangle$$

Jayne and St Laurent, 2001

Energy conversion from barotropic to baroclinic tide, from parameterization.

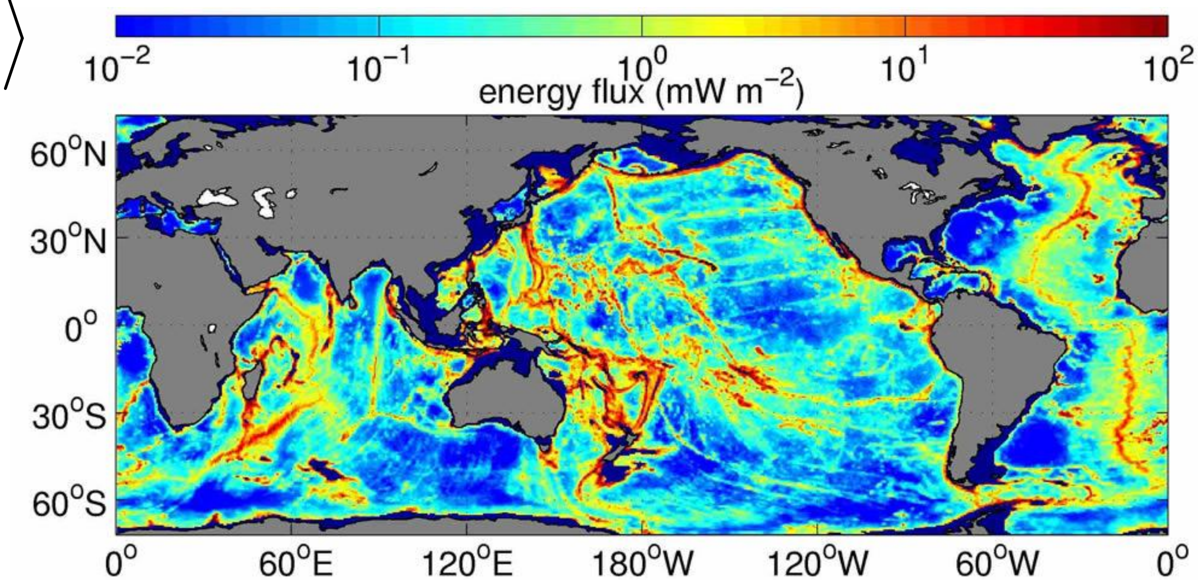

Energy loss from M2 tide, deduced from Topex-Poseidon SST: frictional dissipation in shallow seas, conversion to baroclinic tide in deep ocean.

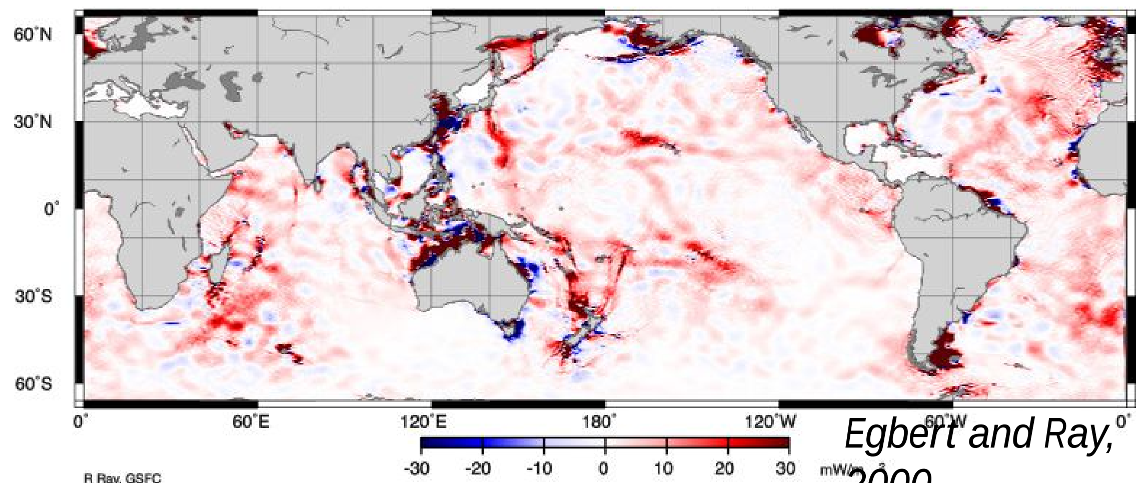

Egbert and Ray, 2000

Extensions to energy conversion theoretical predictions

Generalize linear theory for arbitrary topographic shape and finite ocean depth H

$$P = \int E_f \, dx = \frac{2}{\pi} \rho_0 \sum_{j=1}^{\infty} \sum_{n=1}^{n_0} n\omega \left[\left(N^2 - n^2\omega^2 \right) \left(n^2\omega^2 - f^2 \right) \right]^{1/2} \frac{|\hat{h}(k_{jn})|^2}{j} J_n^{\,2}\left(\frac{U_0 k_{jn}}{\omega} \right)$$

$\hat{h}(k_{jn})$ =fourier transform topography

$$k_{jn} = \frac{j\pi}{H} \left[\frac{n^2\omega^2 - f^2}{N^2 - n^2\omega^2} \right]^{1/2}$$

Resonant wavenumbers

Khatiwala (2003), Llewellyn Smith and Young (2002)

Steep topography: $\gamma \geq 1$

Relaxing linearization of bottom boundary condition (but retaining linearized NS eqns) *(Balmforth and Peacock, 2009)*

Normalized energy flux

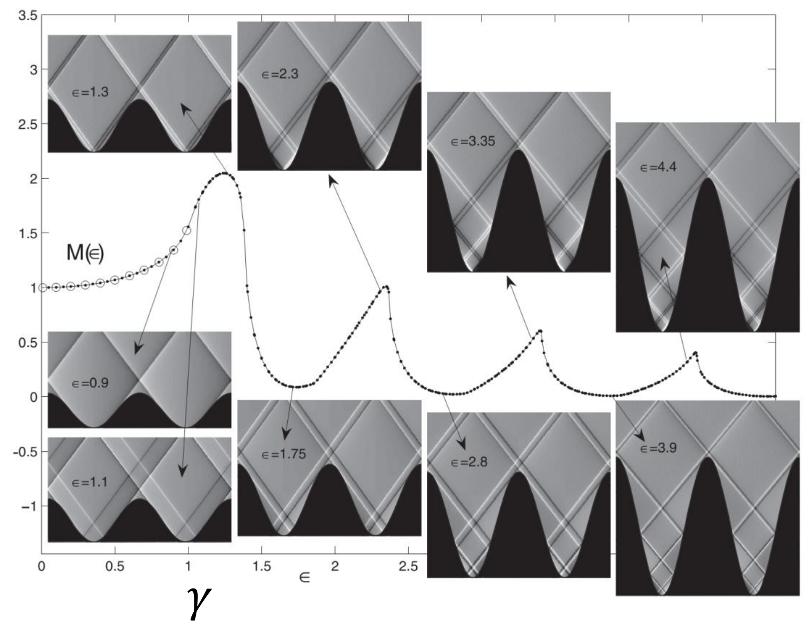

Suppressed energy conversion for steep topography included in global parameterization of tidal mixing at small-scale abyssal hills by *Melet et al, 2013*.

Examples of solutions in linear regime

U_0=2cm/s

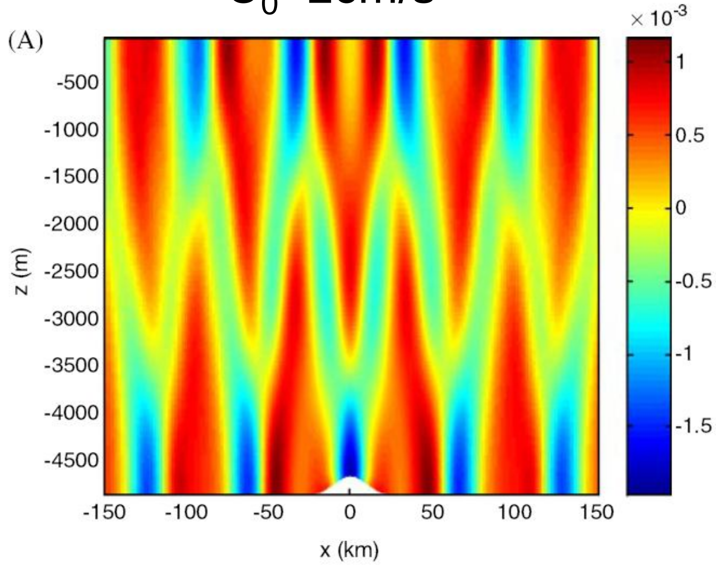

U_0=24cm/s

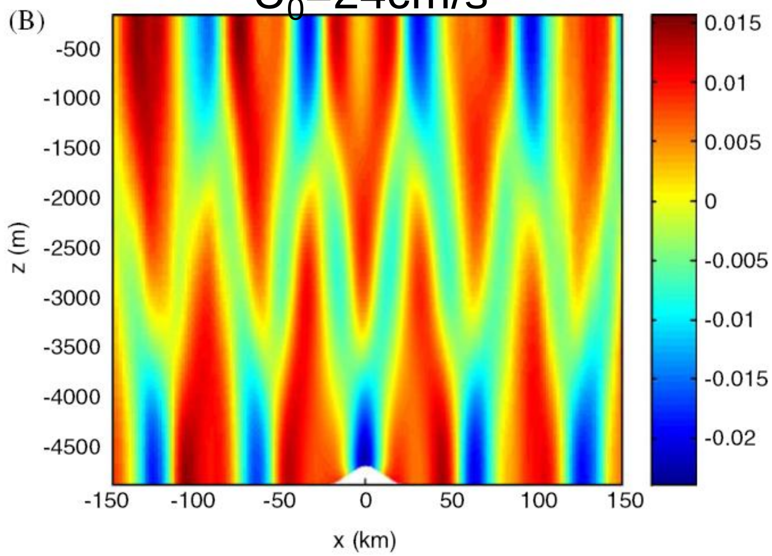

Baroclinic horizontal velocity snapshots

$$h = h_0 \exp\left(\frac{-(x - x_0)^2}{2L^2} \right)$$

h_0=200m, L=10,000m

H=4700m,ω=1.41s^{-1}

Vertical velocity power spectrum

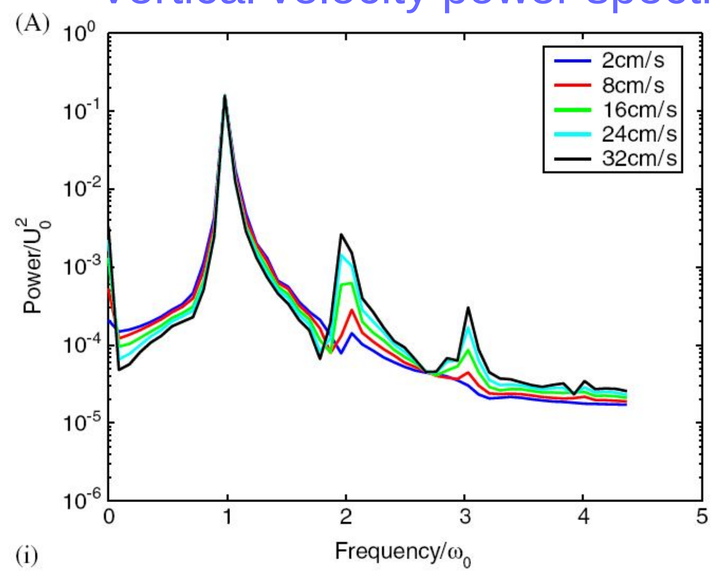

For $U_0/(\omega L)$<<1, spectrum is dominated by forcing frequency

Simulations with MITgcm, Legg and Huijts, 2006

Examples of solutions with $\gamma > 1$, increasing RL=U/(L ω): Generation of higher harmonics

Baroclinic velocity snapshots for low, narrow topography *(Legg and Huijts, 2006)*

RL = 0.35

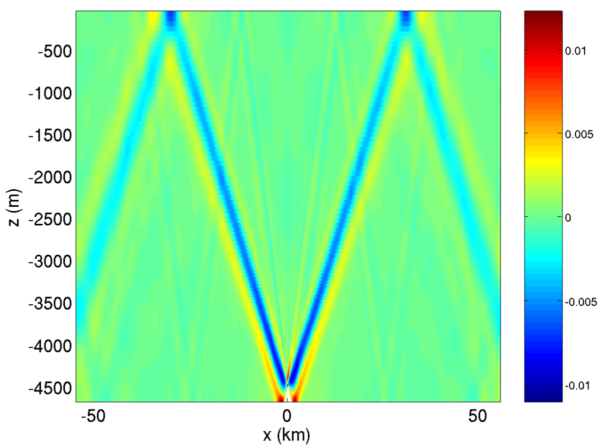

U0=2cm/s

RL = 1.4

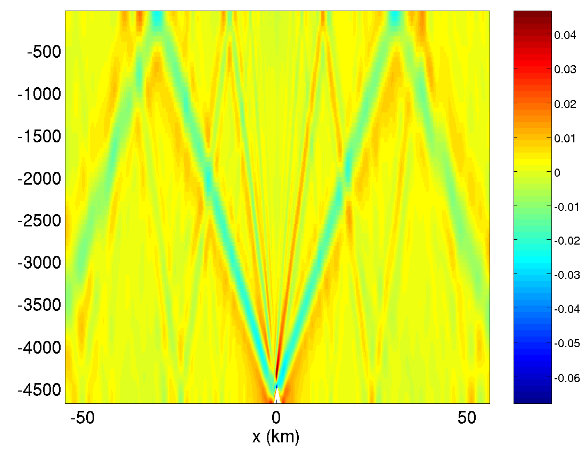

U0=8cm/s

RL = 2.8

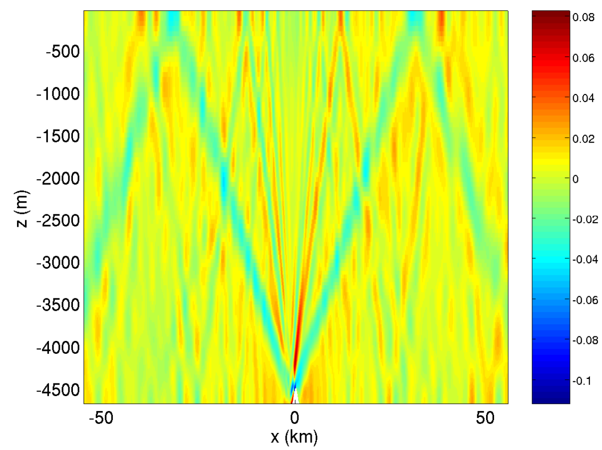

U0=16cm/s

More beams, at steeper angles, corresponding to 2ω, 3ω, 4ω appear as U0 increases.

Actual power spectra

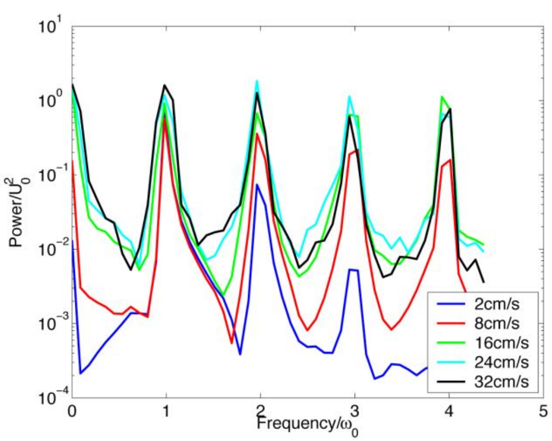

Theoretical power spectra

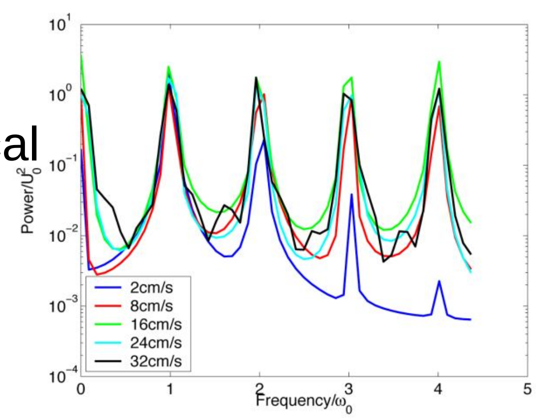

Linear theory (Bell, 1975) predicts higher harmonics well

When and where do tidally-generated internal waves break?

- Linear theory can provide a guide to the energy converted from barotropic tide to internal waves, but turbulence and mixing only occur if the waves break – a nonlinear process.
- Waves break if $Fr = \frac{U}{c} > 1$ or $Ri < O\left(\frac{1}{4}\right)$
- Waves can break if amplitudes increase or vertical length-scales decrease.

Numerical simulations are essential for understanding the fully-nonlinear wave-breaking regime

$$\varepsilon = \frac{1}{\rho} E(x, y) \cdot q \cdot F(z)$$

First, focus on wave breaking at generation site: q, F(z).

Local dissipation at small amplitude rough topography

Diffusivity inferred from microstructure observations (Brazil Basin)

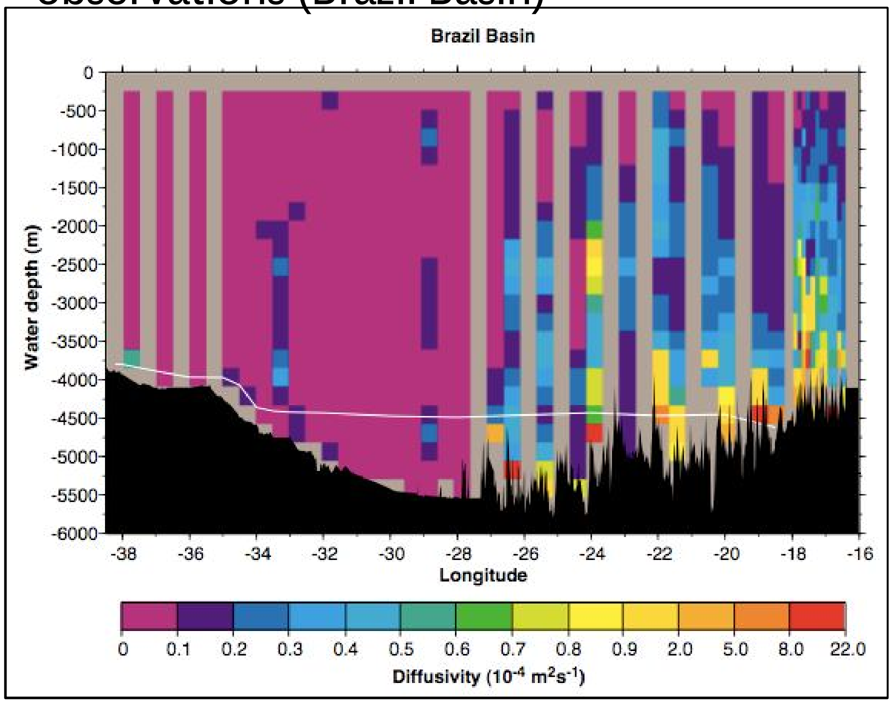

$$\kappa_\rho = \frac{\Gamma \varepsilon}{N^2}$$

(Polzin et al, 1997)

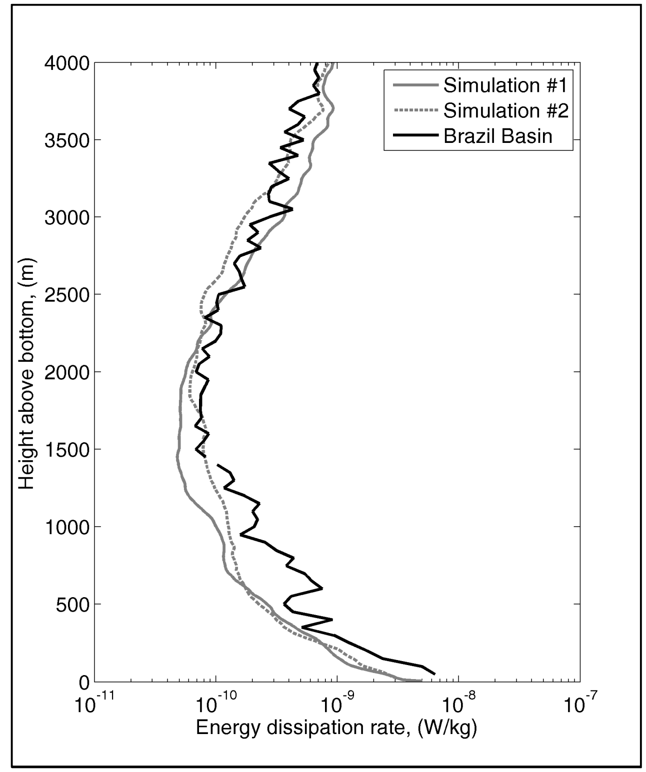

Comparison between observed and simulated dissipation for tidal flow over rough topography *(Nikurashin and Legg, 2011).*

What is responsible for mixing well above bottom boundary?

Local dissipation at small scale rough topography: wave-wave interaction

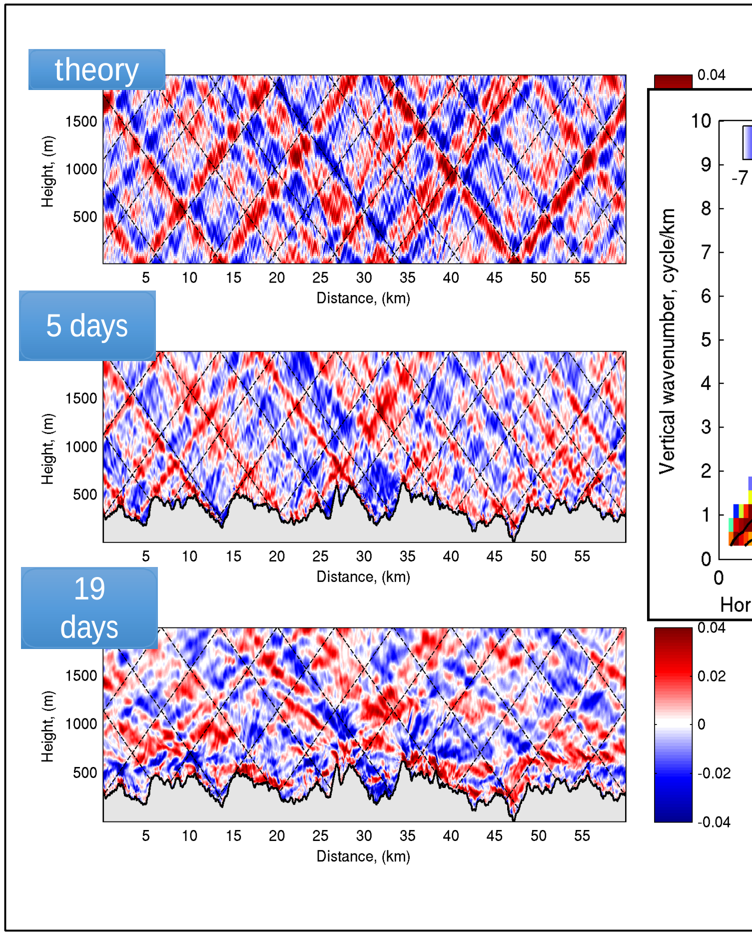

Wave zonal velocity (ms^{-1}): linear solution (Bell, 1975) (top), snapshots after 5 days (middle) and after 19 days (bottom) of simulation.

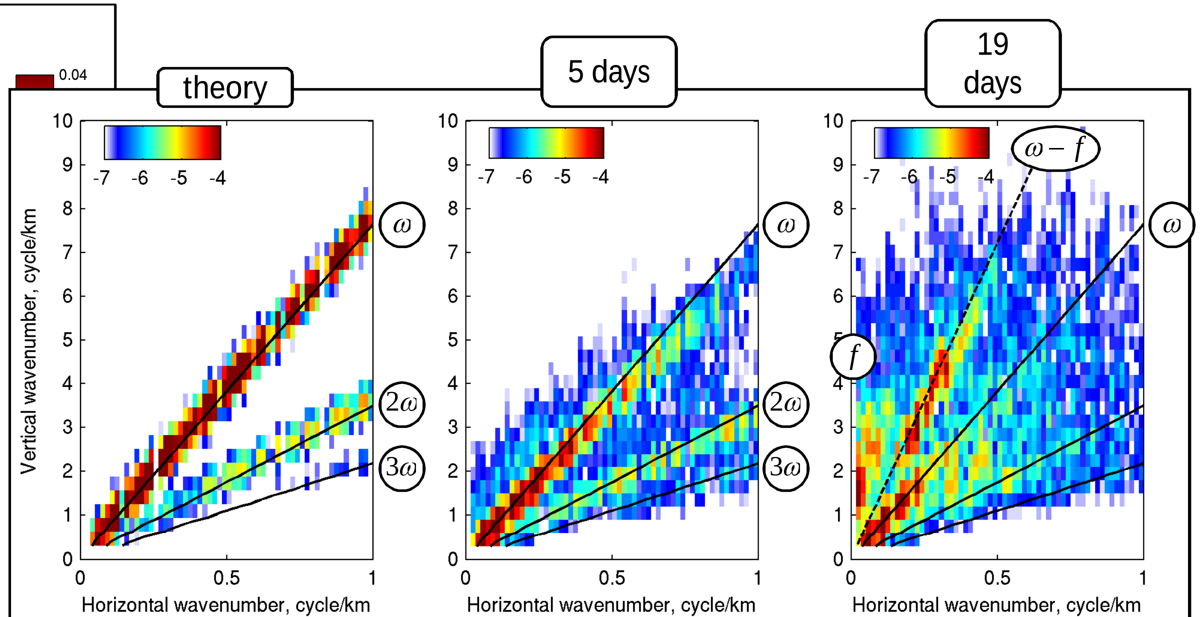

Wavenumber spectra: linear solution (Bell, 1975) (left), after 5 days (middle) and after 19 days (right) of simulation.

Energy is transferred from fundamental frequency ω to lower frequencies f and ω–f.

These frequencies may have higher vertical wave numbers and hence greater shear.

Nikurashin and Legg, 2011

Local dissipation at small-scale rough topography:

Dissipation is enhanced by wave-wave interactions

Dissipation profile is sensitive to Coriolis and topographic wavelength (constant forcing and topographic height)

Horizontally and temporally averaged dissipation

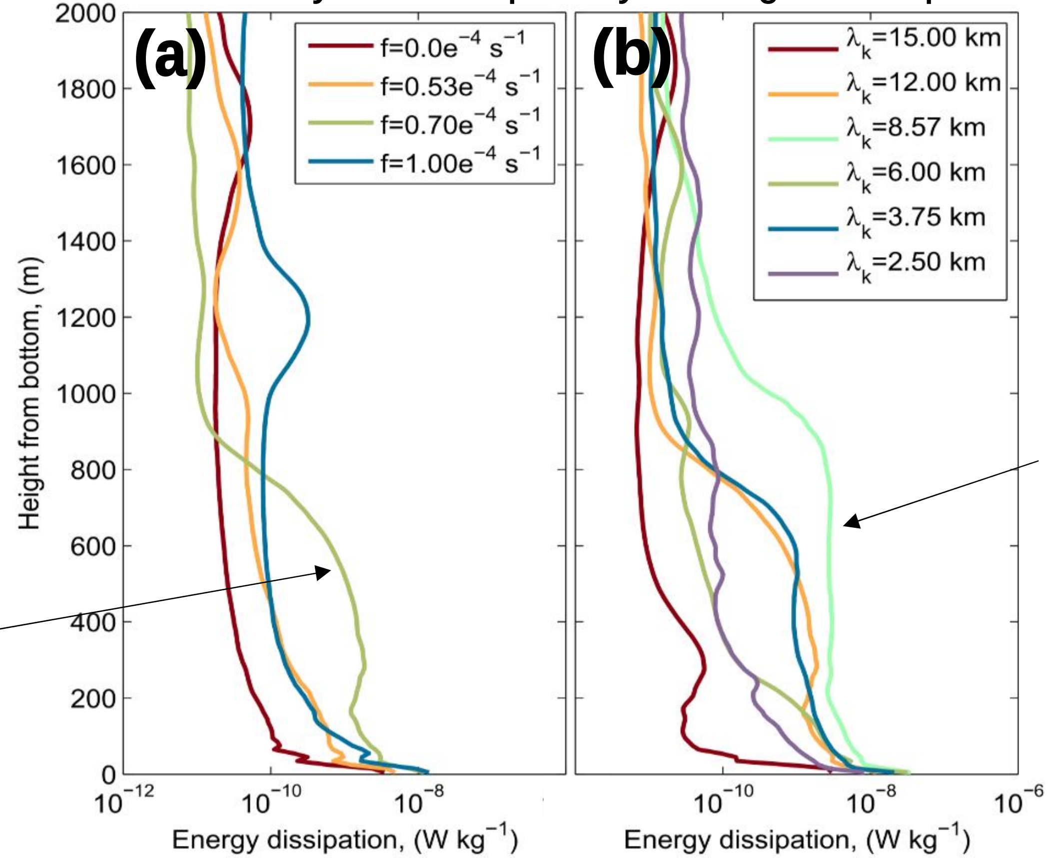

Enhanced dissipation at critical latitude (f = $\omega/2$)

Non-monotonic dependence on wavelength

Fixed topographic wavelength (λ =12km)

Fixed Coriolis (f=$7 \times 10^{-5} s^{-1} = \omega/2$)

(Yi, Legg and Nazarian, 2017)

Local dissipation at small-scale rough topography:

Wave-wave interaction regimes depend non-monotonically on topographic steepness

No rotation $f = \omega/2$

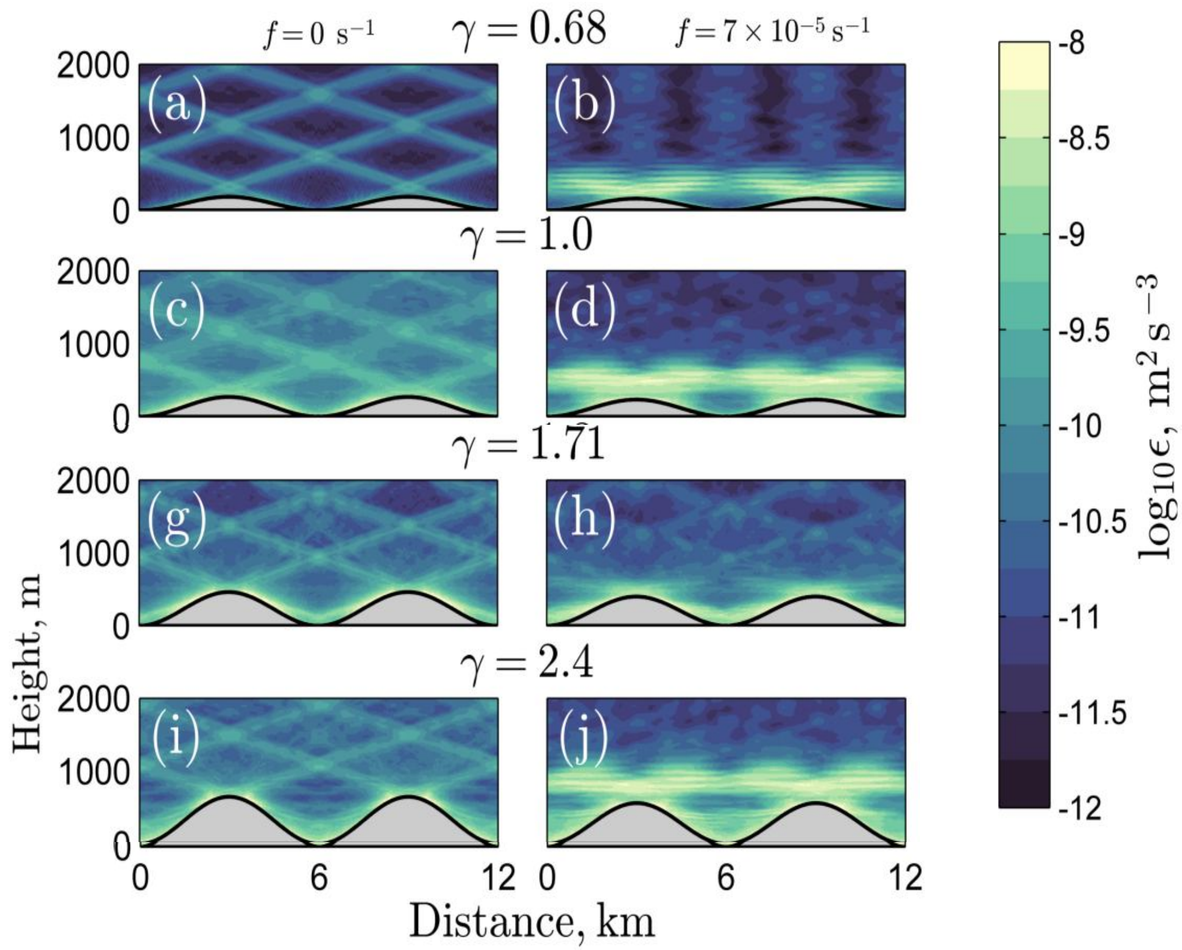

Subcritical slope

Critical slope

Supercritical slope

$\gamma = \nabla h / s$=relative steepness

$s = \sqrt{\frac{\omega^2 - f^2}{N^2 - \omega^2}}$= wave steepness

No enhancement of dissipation at critical latitude when $\gamma = 1.71$

Wave-wave interactions reduce Richardson number at critical latitude

Little increase in low Richardson number region for γ=1.71

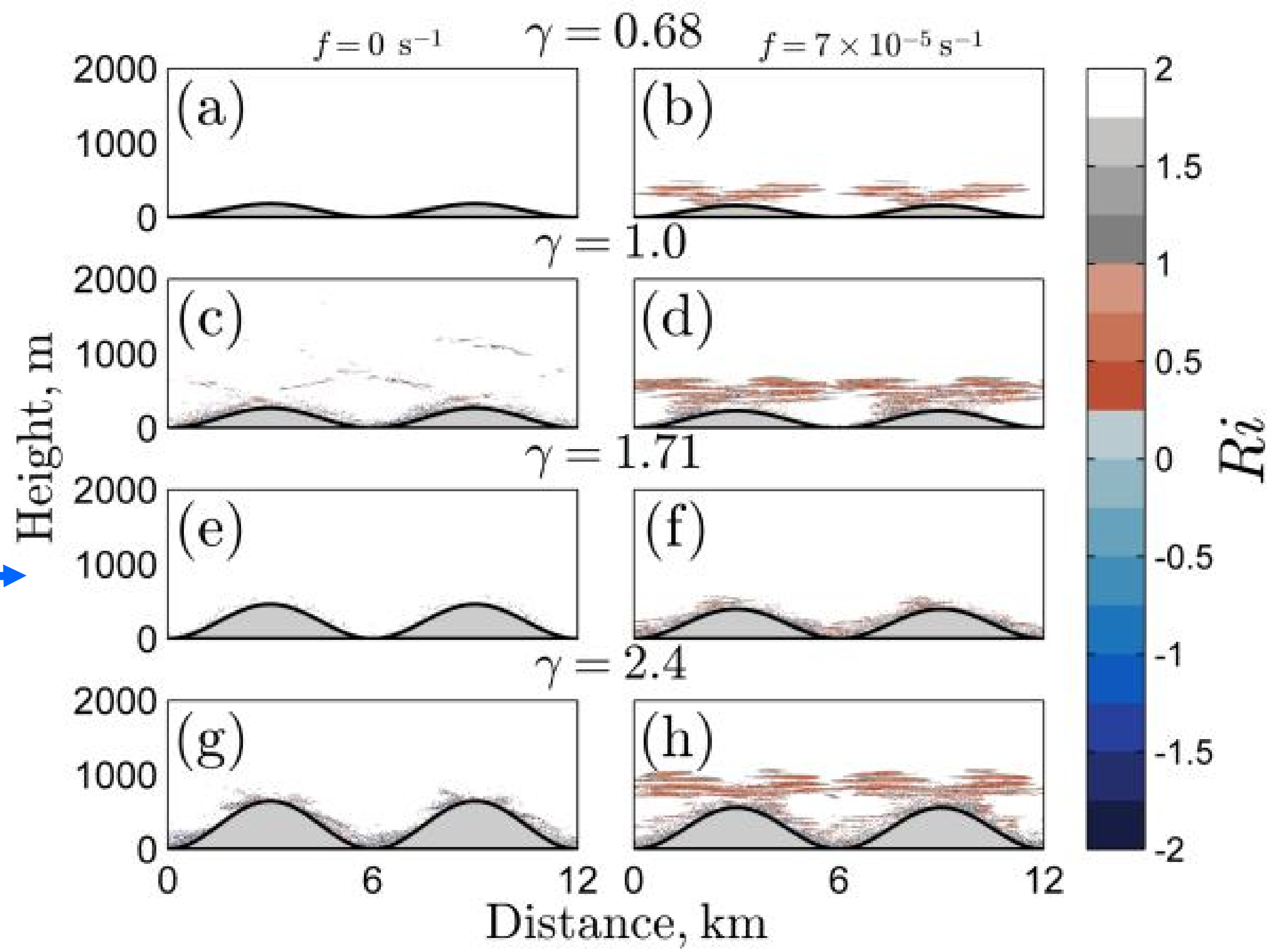

Local dissipation at small-scale rough topography:
Wave-wave interaction regimes depend on topographic steepness

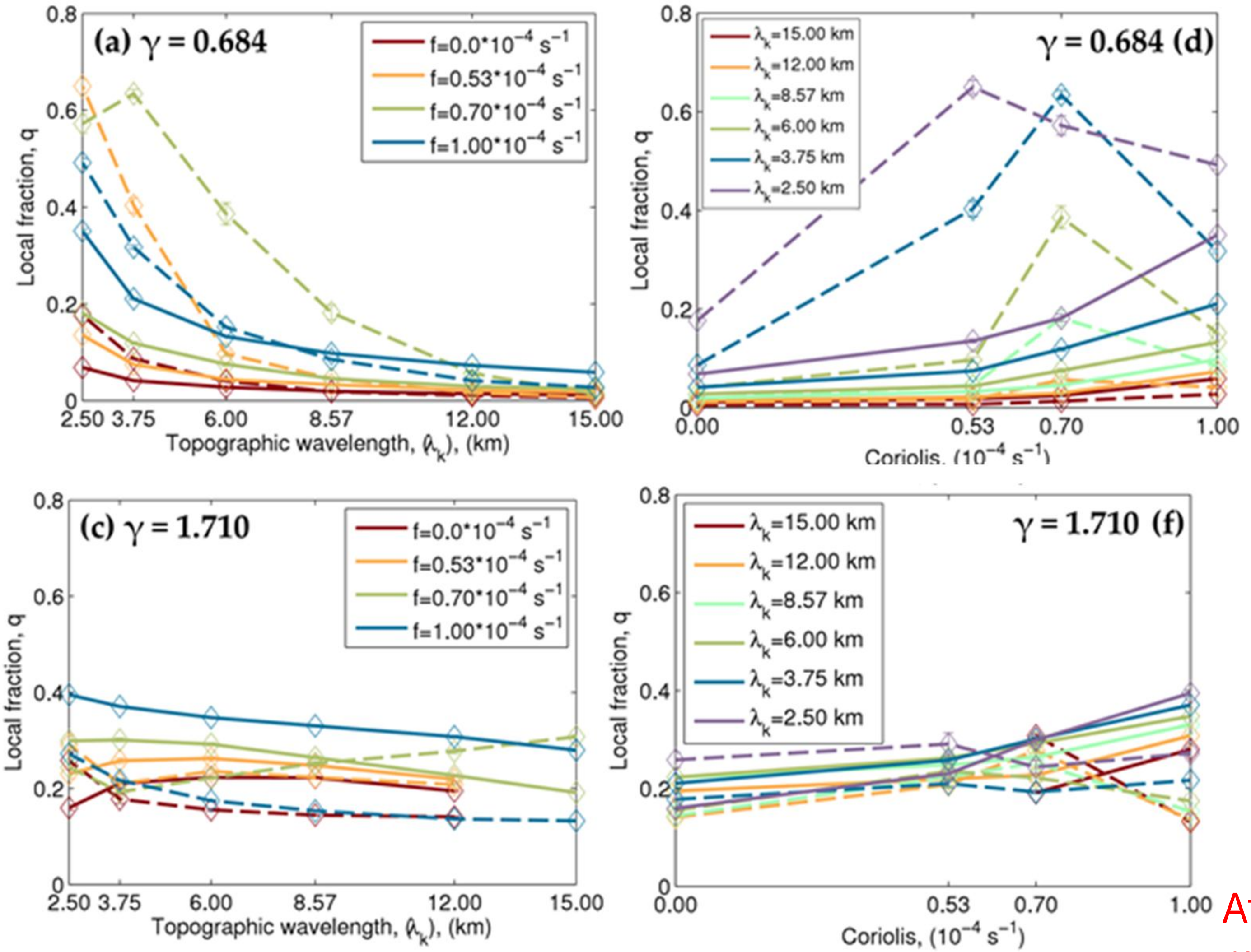

Subcritical topography: dissipation decreases with increasing wavelength, peaks around critical latitude.

Supercritical topography: little dependence of dissipation on wavelength or Coriolis.

At subcritical topography, resonant triad interactions at critical latitude lead to enhanced dissipation.

$$q = \frac{dissipation}{energy\ conversion}$$ =fraction of energy dissipated locally

Local dissipation: internal wave breaking near a tall steep generation site

Observed dissipation at Hawaiian ridge

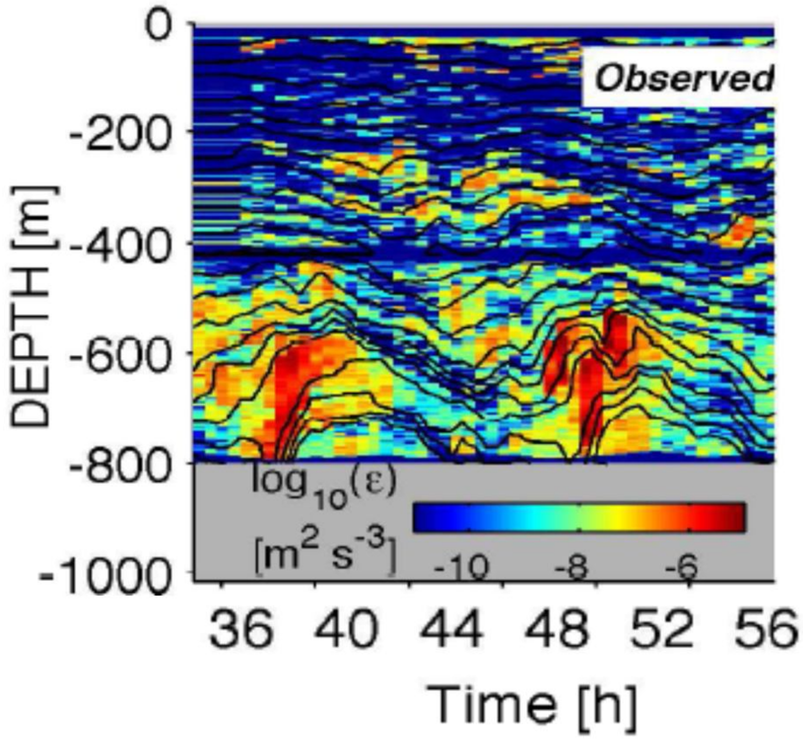

Klymak et al, 2008

Buoyancy field forced by M2 barotropic tide

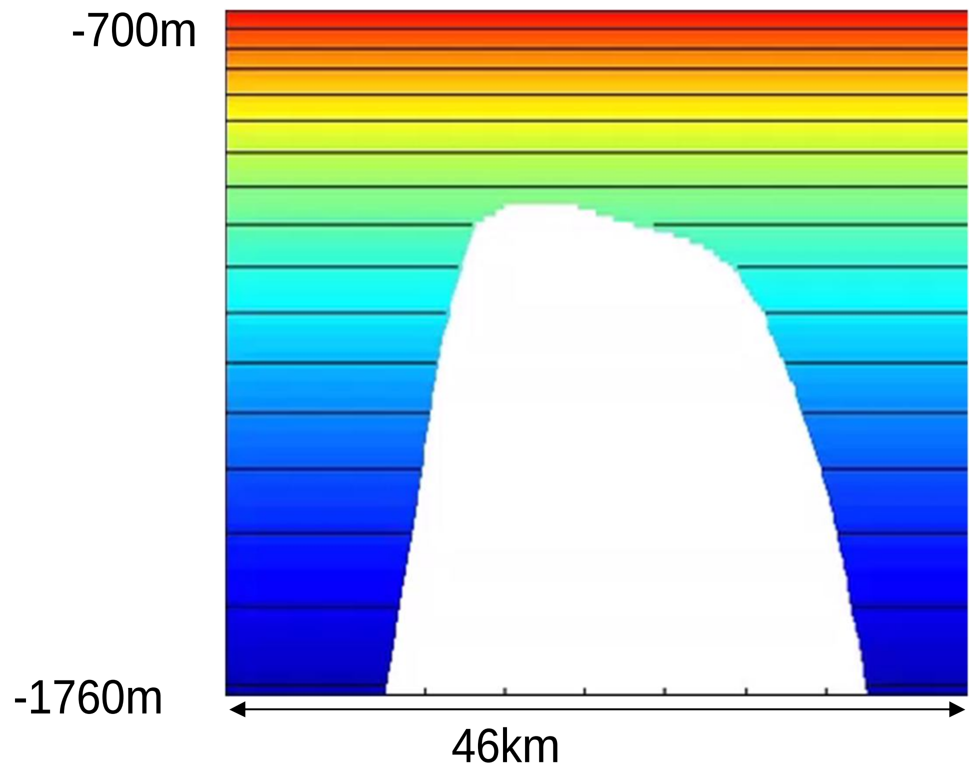

Legg and Klymak, 2008

Wave breaking occurs in transient internal hydraulic jumps, when $\gamma > 1$, and topography is large: $Nh/U > 1$

Local dissipation at a tall steep generation site

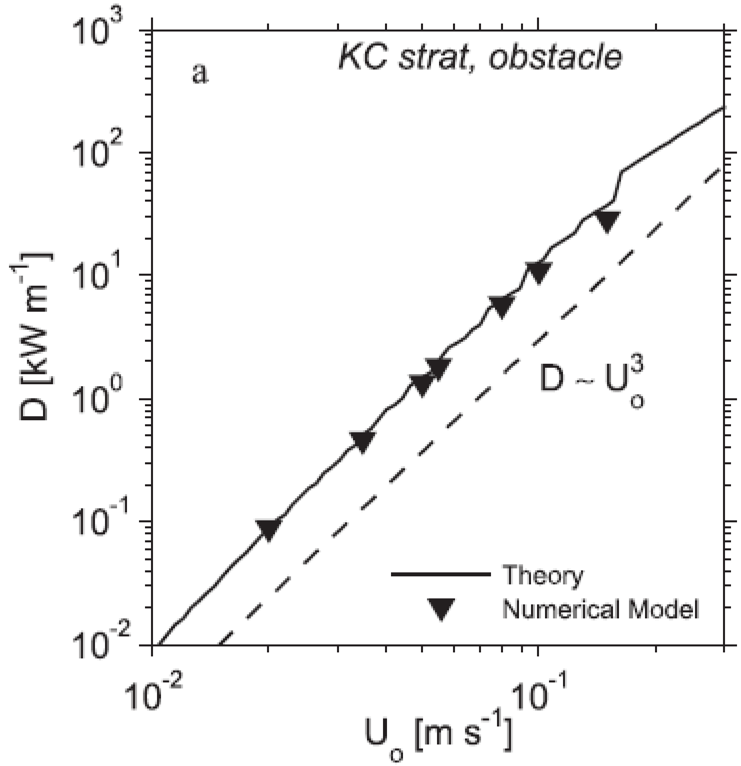

Dissipation scales like U^3 (not U^2 as predicted by St L et al 2002).

$$q = \frac{local\ dissipation}{energy\ conversion} \sim U$$

(Klymak, Legg and Pinkel, 2010)

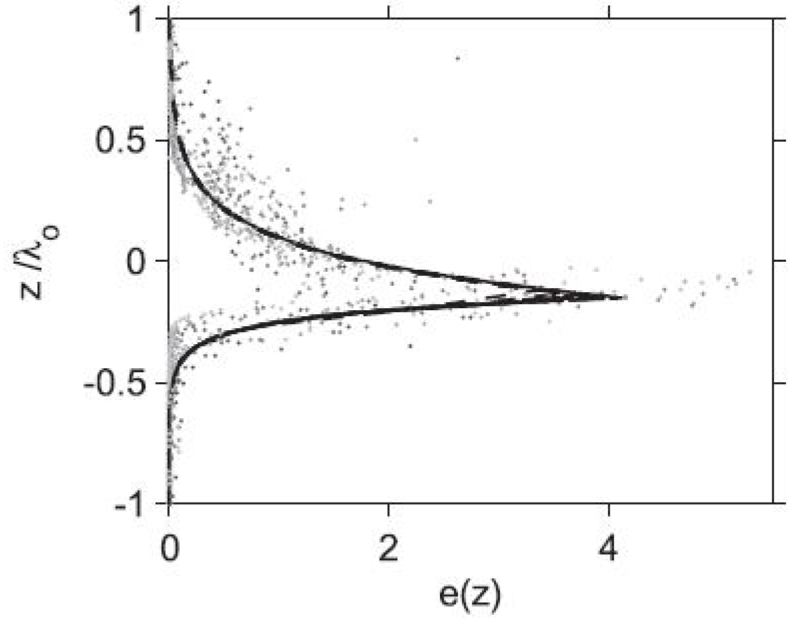

Horizontally integrated dissipation

F(z): vertical distribution decay scale is proportional to $\lambda_0 = 2\pi U/N$. Dissipation maximum located $-0.15\lambda_0$ below the topographic peak; decays exponentially above and below.

Local dissipation at tall steep topography: Interaction between neighboring ridges

2D simulations at west ridge : transient arrested waves

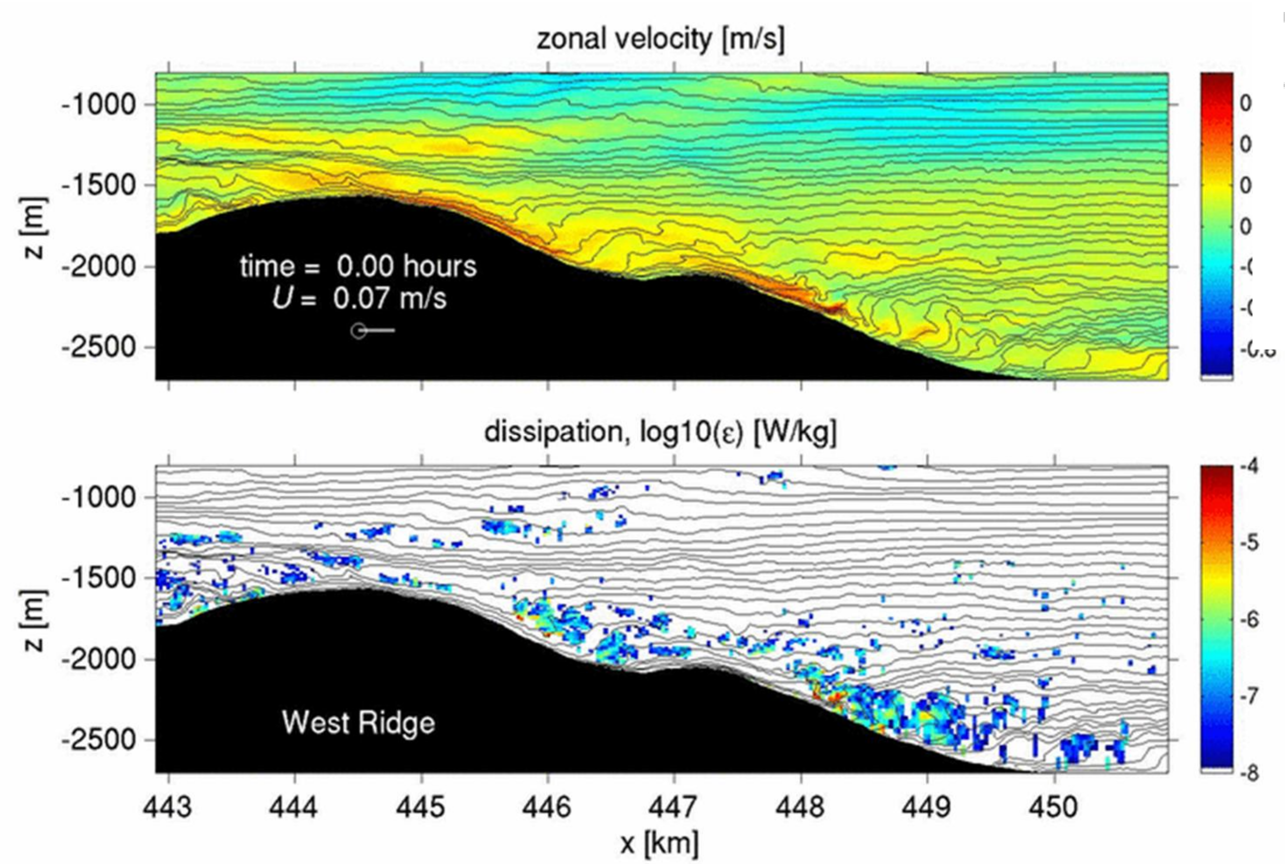

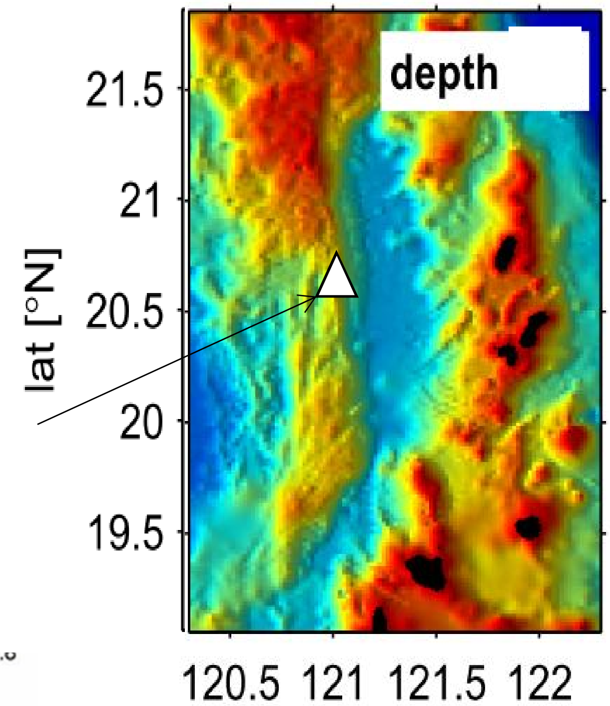

Buijsman et al, 2012, 2013

What happens to propagating low modes?

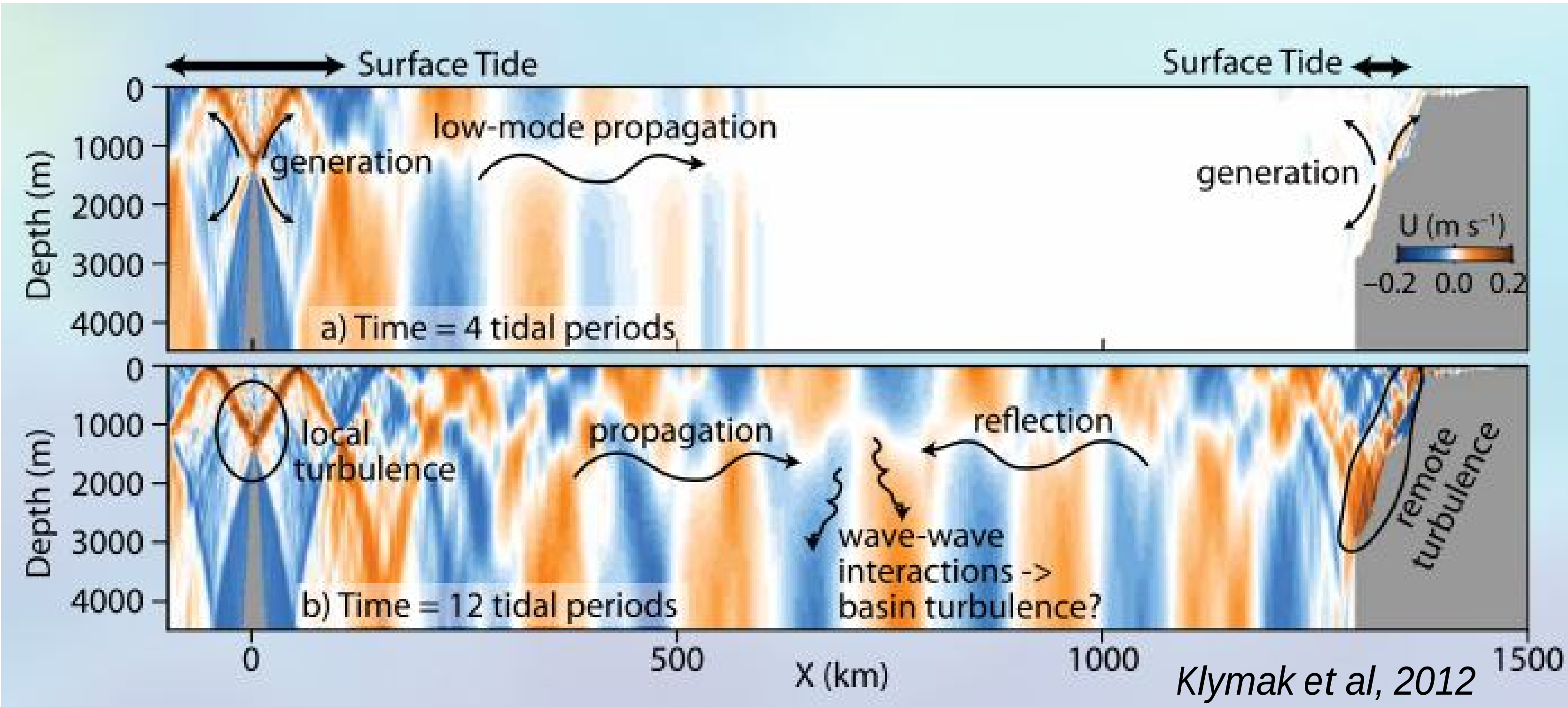

Low modes radiate away, possibly eventually scattering from distant topography

Even at Luzon Straits $q = \frac{local\ dissipation}{energy\ conversion} < 50\%$

Most internal wave energy propagates away from generation site

Low-mode scattering from topography: dependence on topographic steepness

Subcritical topography: $\alpha<\theta$
all energy transmitted to shallower water

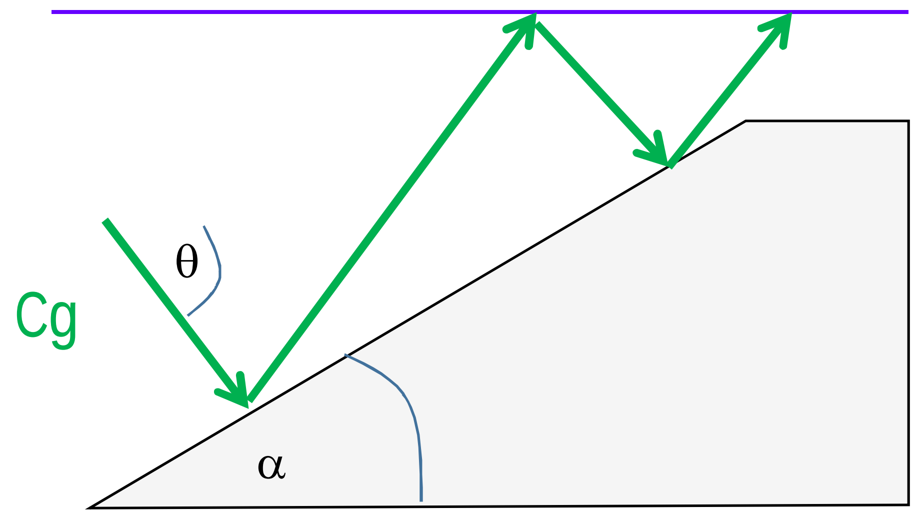

Critical slope:
$\alpha=\theta$: energy incident on slope is scattered into very high wavenumbers along slope.

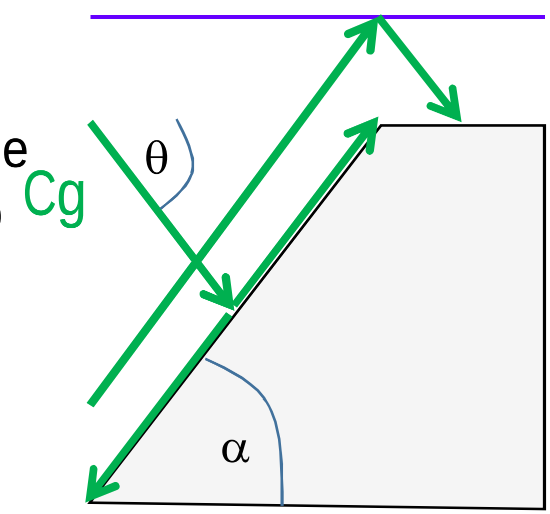

Supercritical topography:
$\alpha>\theta$: energy incident on slope reflected back to deep water.

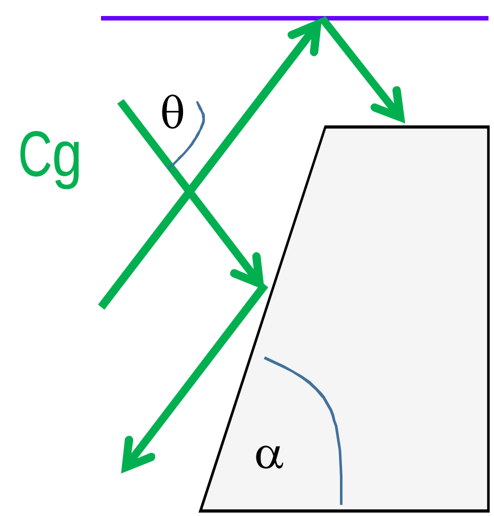

(*Wunsch, 1969; Ivey and Nokes, 1989*)

Low-mode topographic scattering: Supercritical topography

Snapshot of velocity/buoyancy field for mode 1 wave incident on steep ridge.

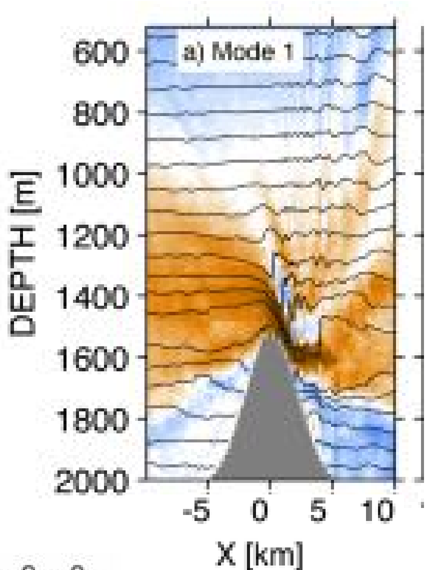

Breaking occurs through transient arrested waves, as at generation site. High modes with Cp< U are arrested, where U is now net velocity amplitude of superposition of incoming, reflected and transmitted waves.

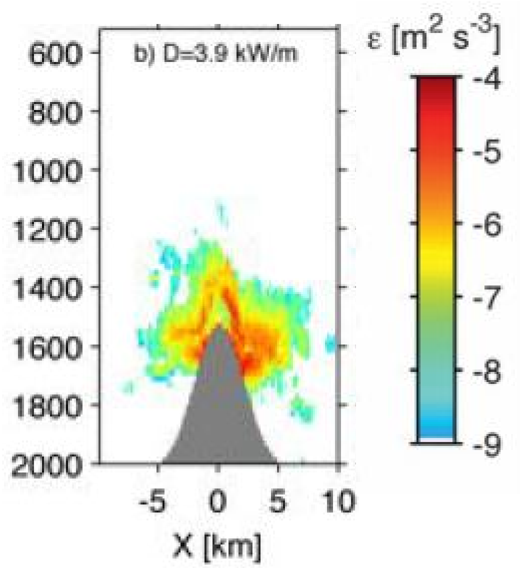

Time-averaged dissipation

Supercritical slopes dissipate < 10% of incoming energy

Fraction of incoming energy dissipated

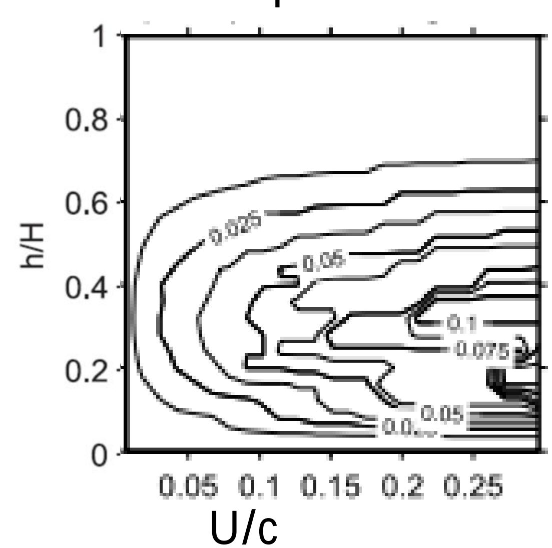

Klymak et al, 2013

Low-mode topographic scattering
Near-critical topography

Critical slope: $\alpha=\theta$: energy incident on slope is scattered into very high wavenumbers along slope.

Dissipation increases approximately linearly with h/H.

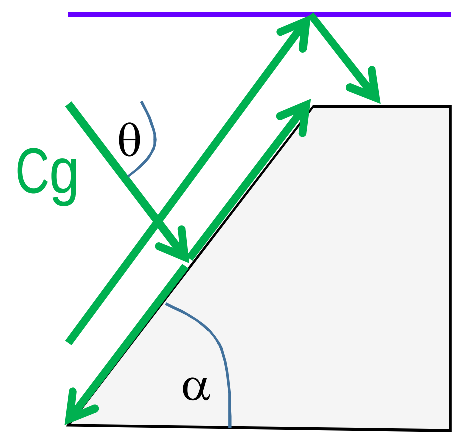

Time-averaged dissipation, scaled by U^2/T (log10 scale)

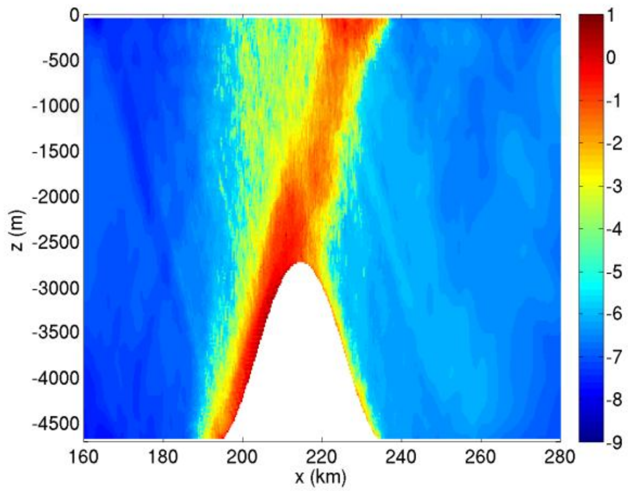

Fraction of incoming energy dissipated

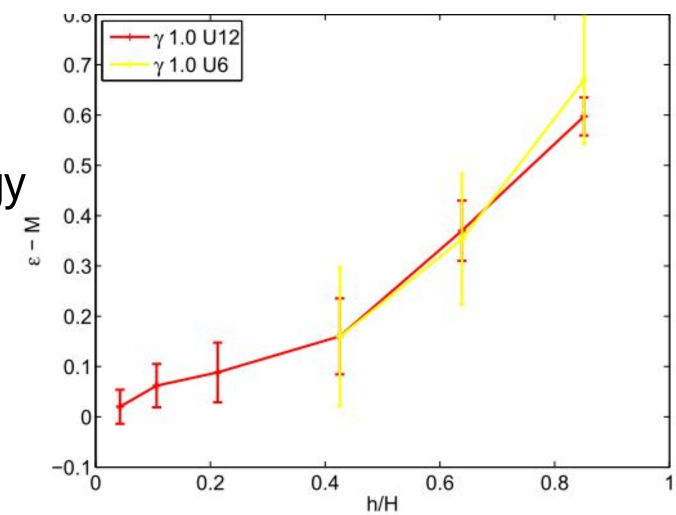

h/H *Legg, 2014*

Up to 100% of incoming energy is dissipated along the slope, independent of wave amplitude.

Low-mode topographic scattering
Subcritical topography

$\theta > \alpha$: All incoming energy is reflected to shallower depths.
Froude number $Fr = U/C_p$ increases as depth decreases.

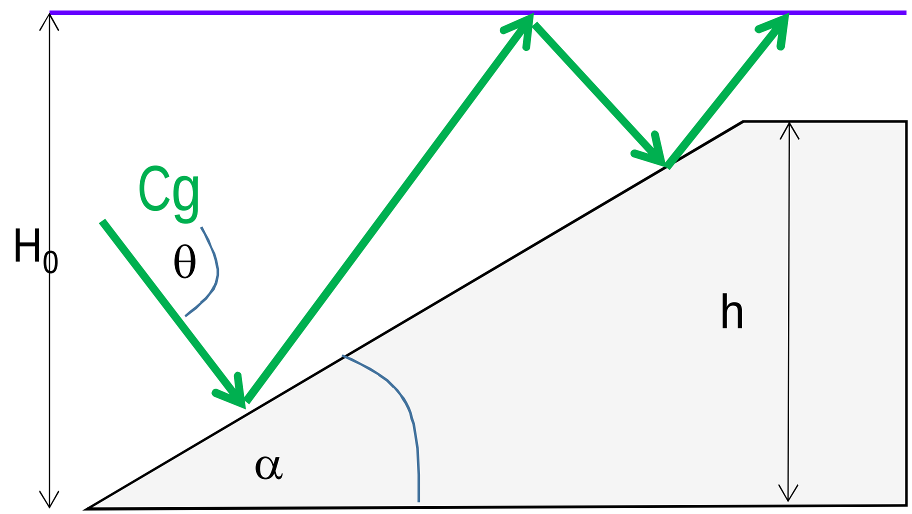

Wave breaks if

$$Fr_{max} = Fr_0 \frac{1}{\left(1 - \frac{h}{H_0}\right)^2} > Fr_{crit}$$

Time-averaged dissipation, scaled by U^2/T (log10 scale)

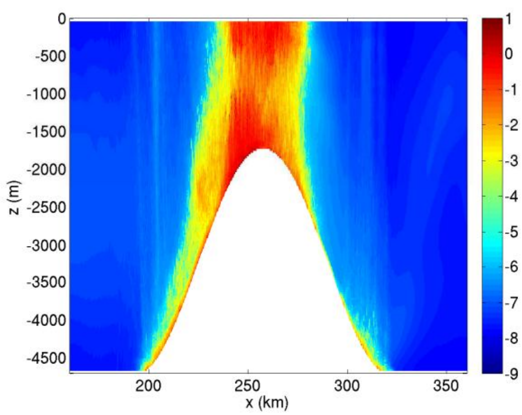

Fraction of incoming energy dissipated

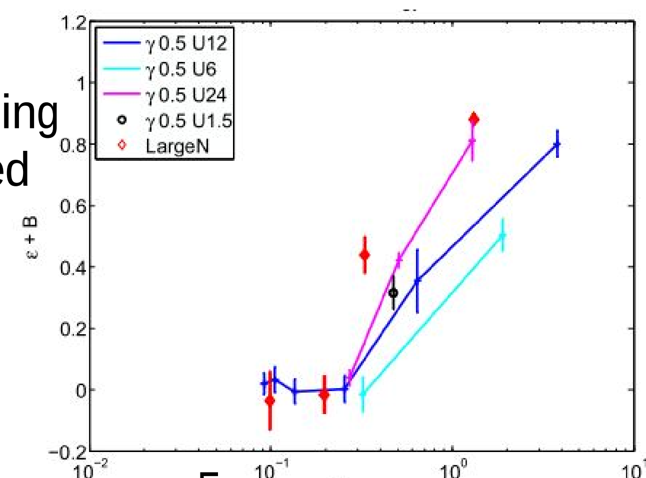

Fr_{max}

Legg, 2014

Up to 100% of incoming energy is dissipated, through whole water column once critical Fr is exceeded.

Does it matter where tidally-driven ocean mixing happens?

Melet et al, 2016

Climate model thought experiment: examine impact of different idealized horizontal distributions of remote dissipation, dividing ocean into 3 zones

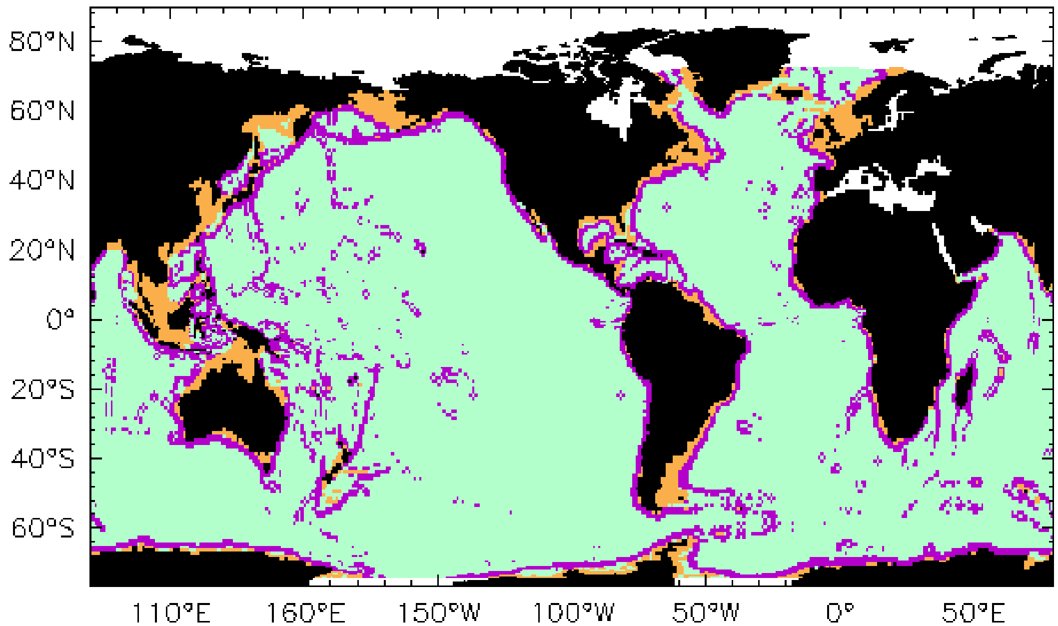

Slopes
Slope > 0.01.
Wave reflection/scattering

Basins
Depth >500m
Wave-wave interactions

Continental shelves
Wave shoaling

Remote dissipation parameterization:
Assign constant value of q_r for each zone

$$\varepsilon_r = \frac{1}{\rho} q_r \frac{E_{global}(t)}{Area_r} F(z)$$

- GFDL ESM2G 1000-year simulations with 1860 forcing include St Laurent et al (2002) representation of local tidal dissipation, with 20% dissipated locally.
- Remaining 80% dissipated in 1 of 3 zones.
- Reference experiment: 20% local, 80% dissipated via uniform $\kappa = 1.4 \times 10^{-5} m^2 s^{-1}$

Influence of horizontal location of mixing on Atlantic Meridional Overturning Circulation

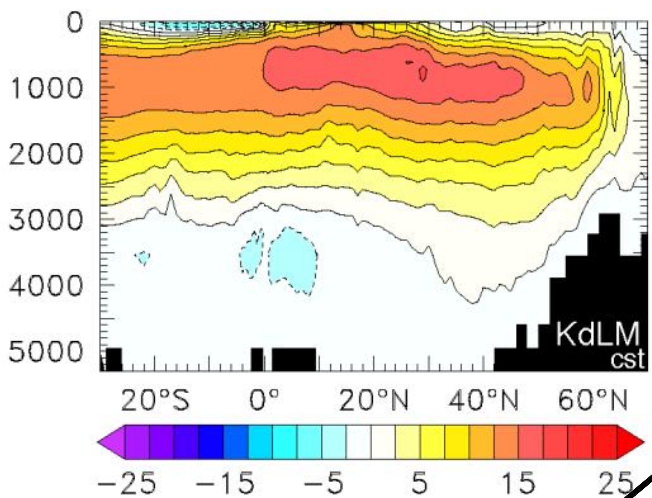

Atlantic MOC (Sv)

Reference: 20% local, 80% uniform diffusivity

- Mixing on shelves/straits weakens AMOC
- Deep mixing strengthens/deepens AMOC

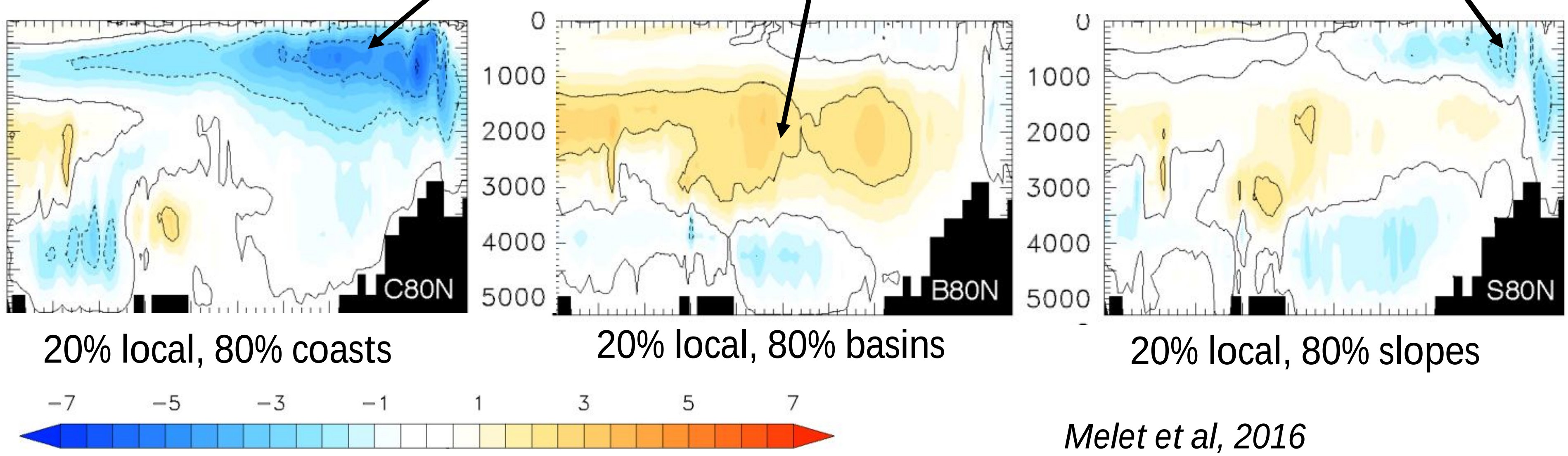

ΔAMOC (Sv)

Melet et al, 2016

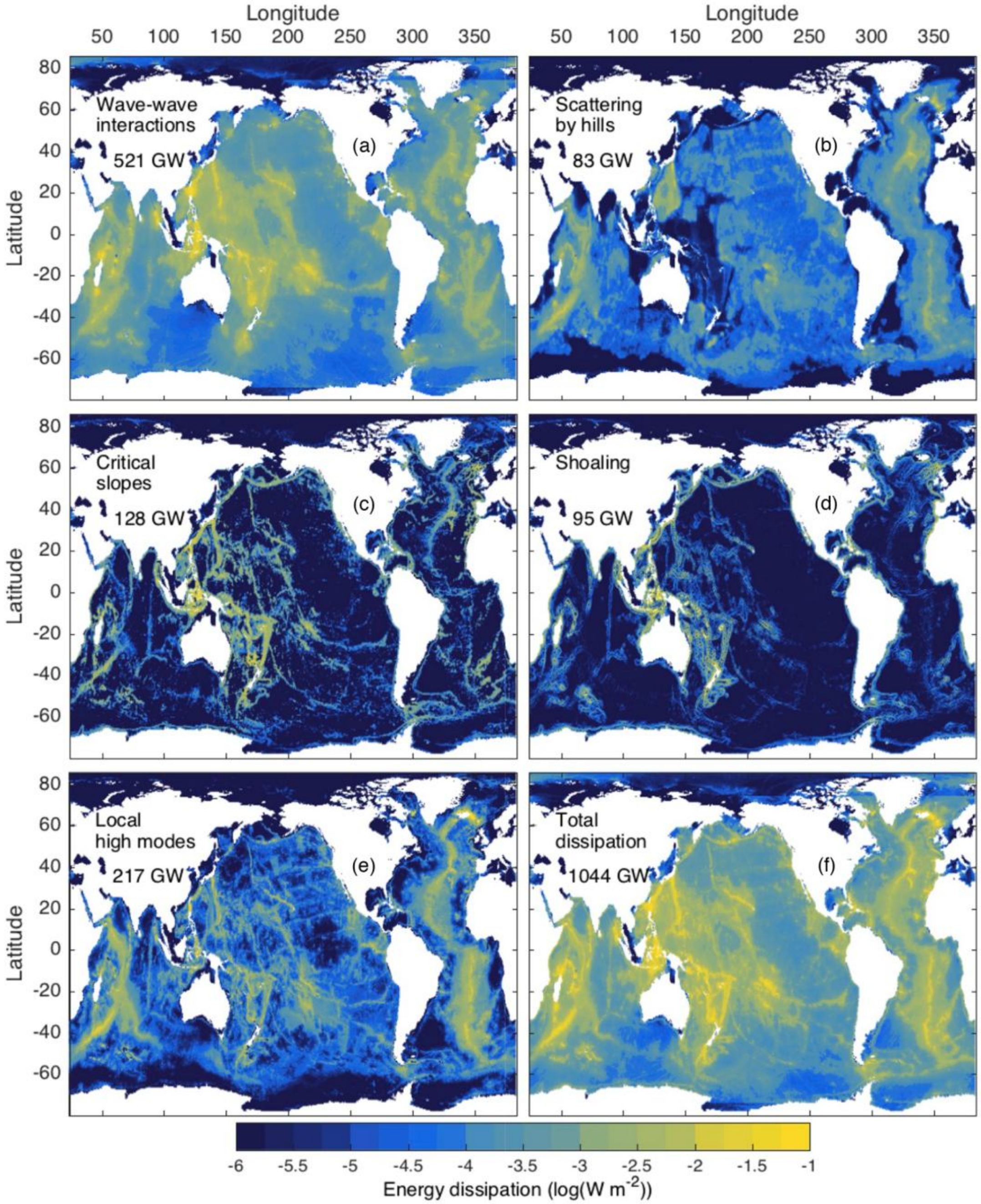

The current best estimate of contributions of different processes to internal tide-driven mixing

(de Lavergne et al, 2019).
Calculated using global 3D ray-tracing and WOCE climatology. Too expensive to calculate during run-time of a global model

Theoretical tidally-generated dissipation compares reasonably well with observational fine-structure estimates of dissipation

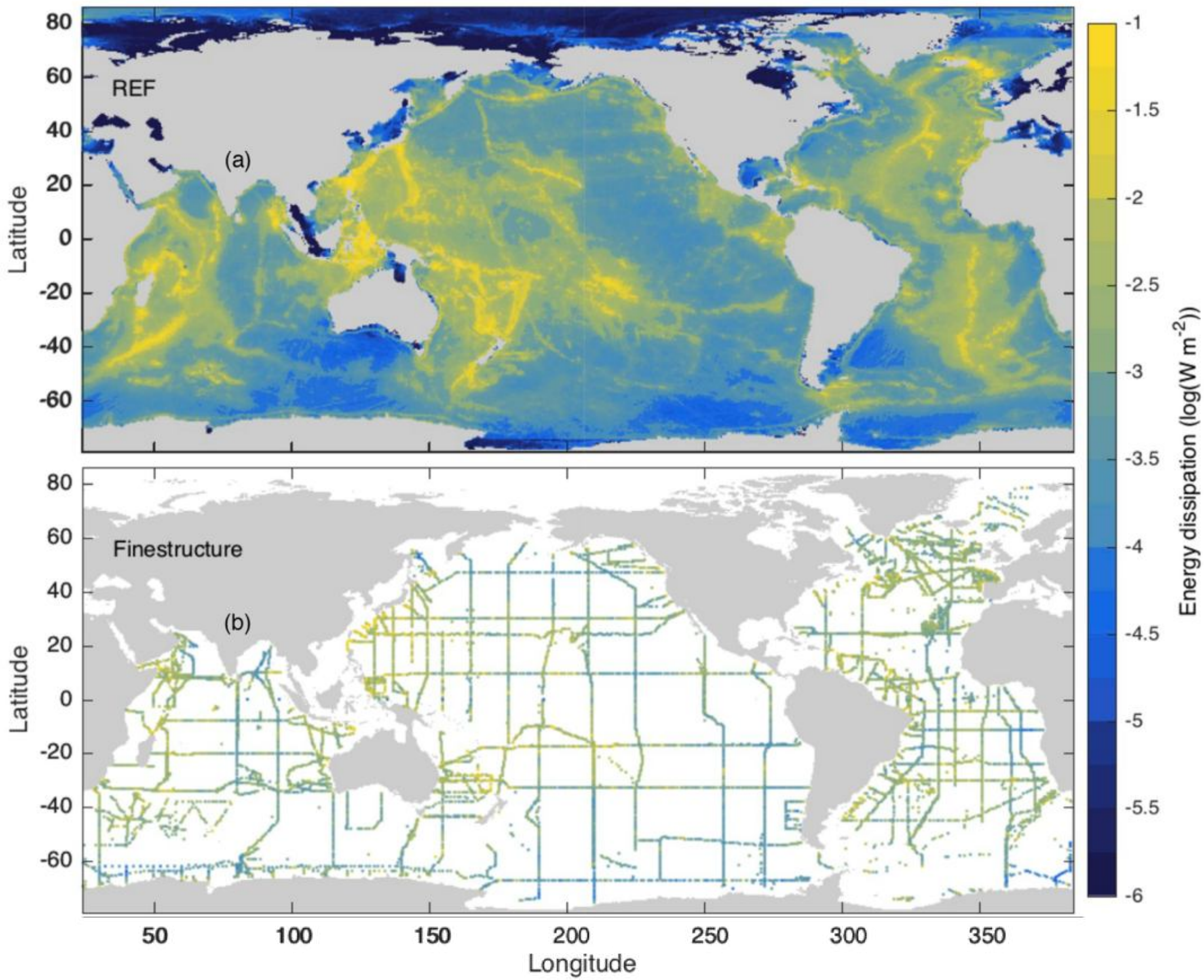

de Lavergne et al, 2019

Kunze 2017

Summary

$$\varepsilon = \frac{1}{\rho} E(x,y) \cdot q \cdot F(z)$$

- Representation of tracer diffusivity in terms of turbulent kinetic energy dissipation- $\kappa = \varepsilon \frac{\Gamma}{N^2}$: allows formulation of an energetically consistent global parameterization
- Energy conversion from barotropic to baroclinic tides: $E(x, y)$: depends on topographic amplitude and shape, tidal flow, stratification
- Local breaking of internal tides: $q, F(z)$: influenced by PSI, transient hydraulic jumps, topographic height and steepness, latitude
- Farfield breaking of internal tides: $(1 - q)$: topographic scattering from continental slope topography
- Toward a global parameterization: $\kappa(x, y, z, t)$: must account for all of the above and more: generation, local breaking, propagation, farfield breaking.
- Impact of tidally-driven mixing parameterizations on ocean circulation and climate: Spatial distribution of tidally-driven mixing can lead to 10-25% changes in AMOC